POLITECNICO DI TORINO

Master's degree course in Automotive engineering

Study and design of an electromechanical parking lock actuator

Supervisor
prof. Andrea Tonoli

Candidate
Andrea Ongaro
Student ID: S253480

In collaboration with Silatech Srl

December 2019

Abstract

Nowadays in the automotive field, the majority of the vehicles are equipped with many actuators of different kind (e.g. eletromechanical, hydraulic, pneumatic) and for different purposes.
In the gear change actuation, in particular for automatic gearbox, is continuosly increasing the use of by wire systems, in which there is not a mechanical connection between the shift knob and the gearbox, but the gear change is realized by means of electronic inputs given by the driver to the shift knob, processed by the ECU and physically applied through the use of actuators.
The purpose of this thesis work is to identify a methodology for the designing phase of an electromechanical actuator based on a customer's specification in which the main function is the engagement and disengagement of the parking lock with an additional peculiar emergency system.
This work has been developed in collaboration with Silatech Srl of Orbassano, a company with a great experience in the gear shift control systems.

Acknowledgements

After so many school years, my academic career has reached the end. Looking back, I can say that there have been tough and joyful moments. I have been lucky, because I have always had by my side special people.

Thanks Danilo, thanks Giuliana, thanks Silvia: you are always my source of serenity. With your sweet and tireless support, both moral and economic, you allowed me to arrive here in front you today.

Since I met a person, my life, in all its aspects, took flight in the right direction: thanks Sveva, you are my reason of happiness and lightheartedness.

Thanks to all my friends (and i repeat, ALL my friends), Emilio Tauro, Iper, Road to, and all the others, you are a fundamental part of this important achievement.

Finally, I would like to express my gratitude to all those people that actively have taken part to the realization of this work: thanks to my supervisor, Andrea Tonoli, and thanks to all my colleagues of Silatech that, in these months, have always encourage and supported me.
A heartfelt thanks to all.

Torino, 2019
Andrea Ongaro

Contents

List of Tables

List of Figures

Chapter 1

Introduction

The shifting mechanisms are undergoing, for some years, a period of change, also due to the increasing of electric cars market.
Nowadays traditional gear shifters, in particular for full automatic gearbox, composed by a mechanical connection with the shift knob, can be modified in order to obtain a system defined "by wire" in which the actual force actuation is moved from the driver hand to an actuator that can be positioned in a midpoint between the transmission and the shift knob, or directly on the gearbox.
In general, it is possible to identify the use of actuator that manage all the gear position(P,R,N,D) or 2 different actuators, one for the gear positions R,N,D and one for the P position, that generally is the position that requires the greater amount of force, this is the reason why is managed separetely by the others.
In this work, the focus will be on an actuator that must be used for the management of the P position realized by means of the engagement and disengament of the parking lock in a dual cluth transmission.

1.1 Gear shift mechanisms

1.1.1 Shift by cable

In fully automatic gearbox, the traditional gear shifter is composed as in figure1.1: in that configuration we have a force actuation that is, with the suitable reduction system, directly applied by the driver's hand. The cable end on the transmission side selects the four different position directly on the gearbox, as represented in figure1.2, by means of translation of the bowden cable.
Differently, in dual clutch gearbox, the cable connection between the shift knob and the gearbox is just used for the parking lock engagement and disengagement

Figure 1.1: Shifter by cable system, Silatech product

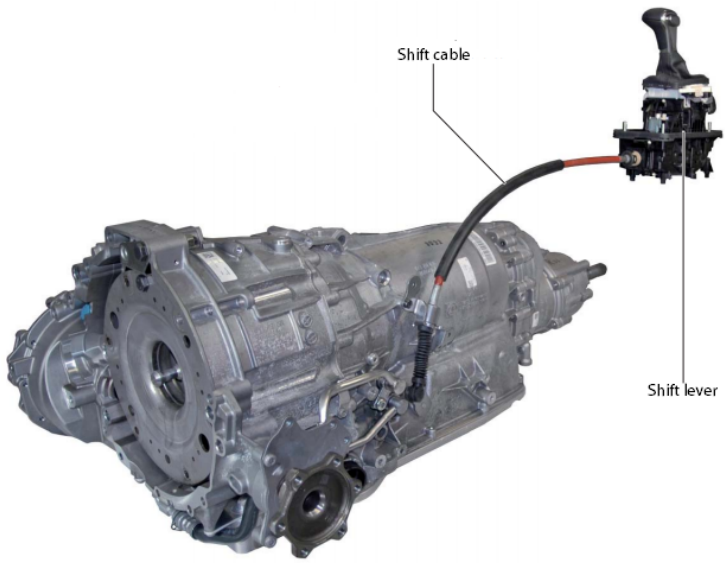

Figure 1.2: Shifter by cable system configuration

and all the other positions are just electronic inputs given to the ECU that, by means of the actuation unit directly installed on the gearbox, is able to manage the gear change.
A configuration like the one just described, can be considered as an hybrid solution between shift by cable and shift by wire.

1.1.2 Shift by wire

In shift by wire systems, the driver gives an input to the shifter, that in this case can be different with respect to a common shift knob, as in figure 1.3, and that input is a complete eletronic input given to the ECU: this is a pure electronic system, therefore the actual selection of one of the four position is assigned to the actuators that could be electromechanical or hydraulic. In figure 1.5 is presented an overview of a by wire system.

Figure 1.3: Shifters for shift by wire systems, Silatech products

So these configurations of shifting need the addiction of actuators, that can have direct or remote mounting: in the latter, the actuator is mounted somewhere far from the gearbox, for example under the shift knob, and due to the distance from the gearbox it is necessary to use a cable from actuator to actuation point, as represented in figure 1.4.

Figure 1.4: Actuator with cable output

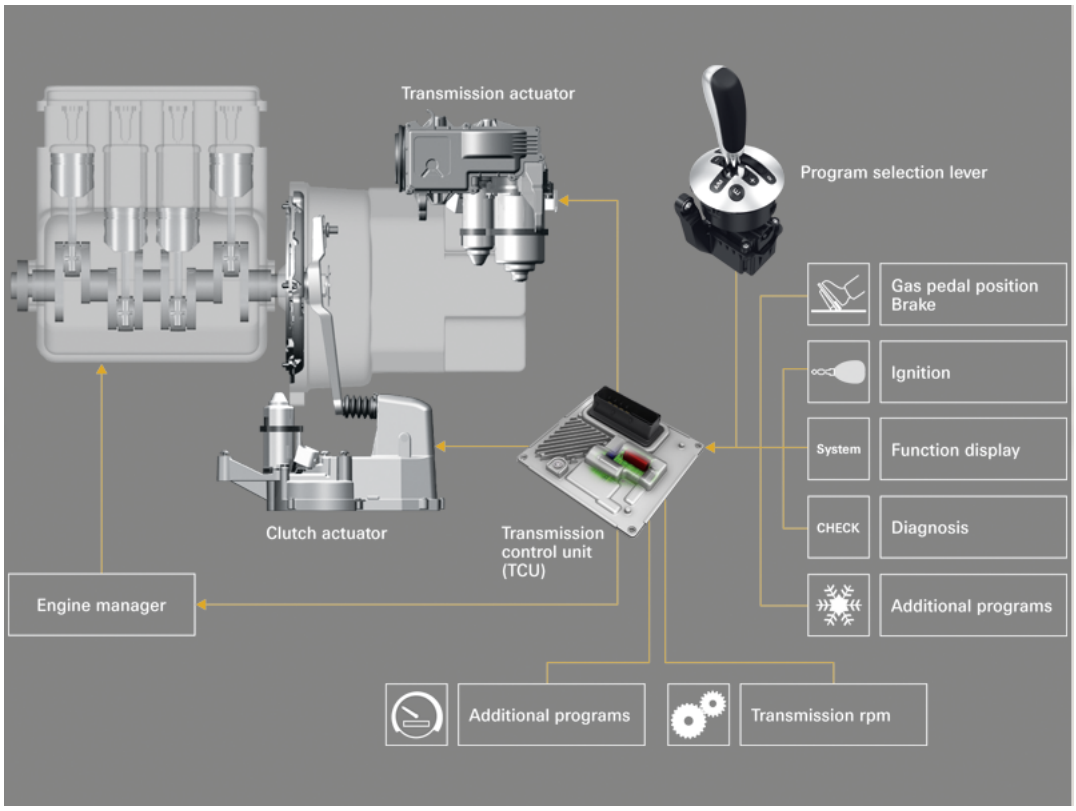

Figure 1.5: Block diagram for gearchange actuation

1.1.3 Parking lock

The parking lock is a system used in automatic transmissions to lock the vehicle and it is used in parallel with the parking brake.
The locking is realized by means of a hook that engages a toothed gear on the differential side, like depicted in figure 1.6.
In dual clutch gearbox generally the bowden cable it's used just for this purpose, because the engagement of the P position requires much more effort with respect to the other positions. An actuation unit is used for the management of those positions, physically mounted on the gearbox, as properly explained in [1].
The engagement and disengagement are actions that depend upon the vehicle conditions: mass on board, road pendence and vehicle mass. The disengagement load generally is the highest one, especially in high road slope conditions, as depicted in figure 1.7: the load is extremely high in the first millimeters of motion, because the system it's in a traction condition and needs to win a great amount of friction force due to the mass and road slope and, subsequently, decreases quite rapidly.

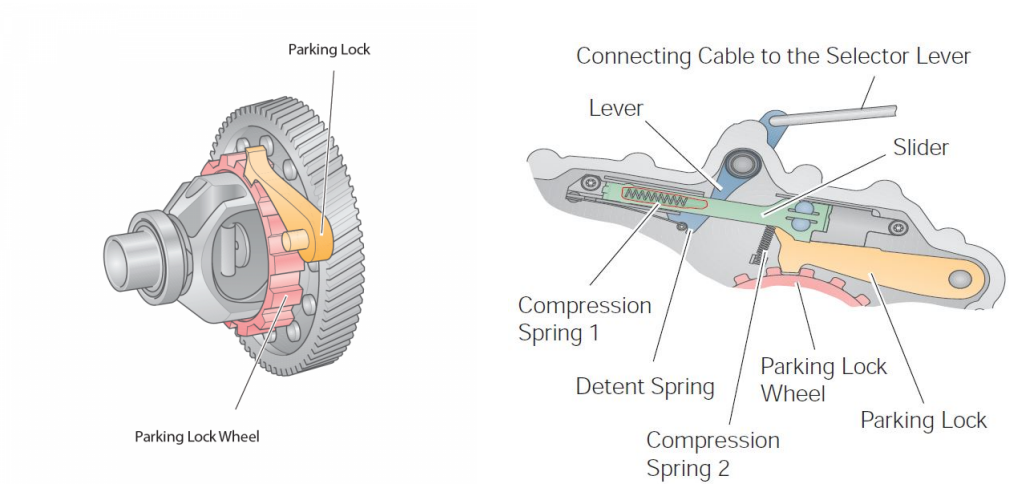

Figure 1.6: Parking lock system

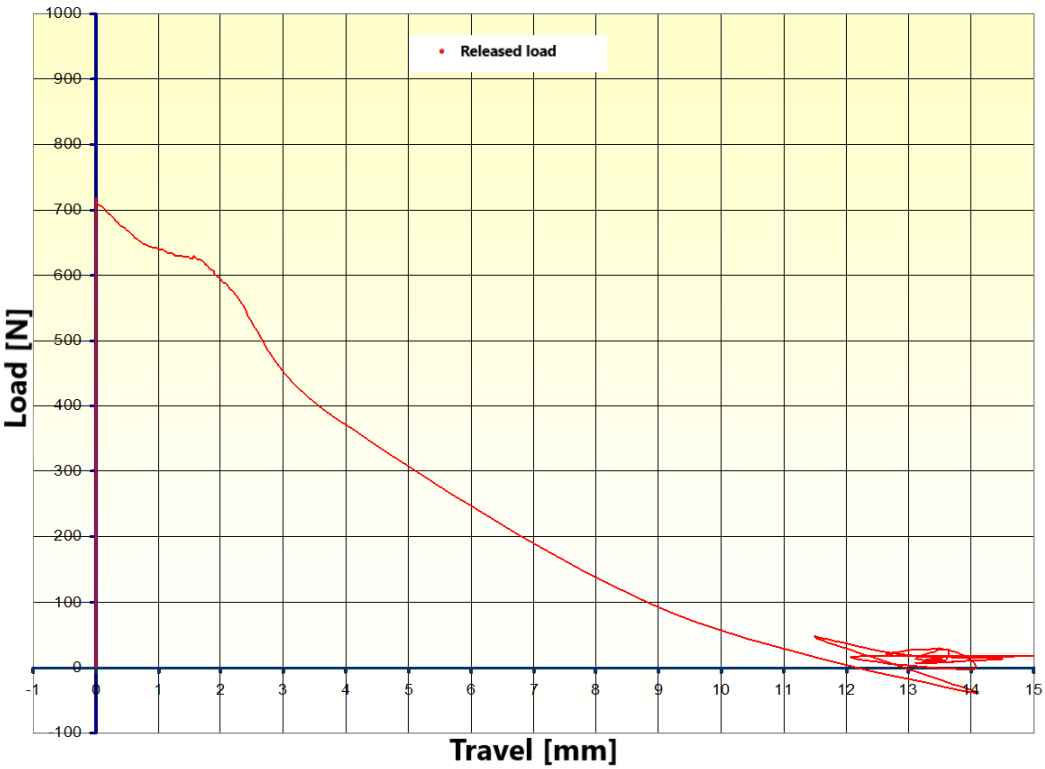

Figure 1.7: Parking lock disengagement diagram example

1.2 Actuators: state of art

Most of the articles and general information available online about electromechanical actuators, and actuators in general, are mainly related to the aeronautic field, due to the general secrecy present around the automotive field; nevertheless this is enough to underline which are the main trends and design methodologies generally used: of course different targets and extremely different load conditions, but similar guidelines.
As stated in [2], the conventional hydraulic actuators are high maintenance and less resistant to high temperatures and pressures: in order ot increase efficiency and reduce costs, electromechanical actuators (power by wire systems) are the right solution.
We can identify more advantages:

- increased safety due to the absence of flammable fluids;
- reduced weight and complexity of power transmission paths;
- easier maintenance;
- higher efficiency and better dynamic characteristics;

The general configuration of an EMA (electromechanical actuator) is shown in figure 1.8(a): of course is needed the electric power supply, an ECU for what concern the data elaboration and control strategies, the servo motor and the gearbox in order to have reduction of speed to reach the torque necessary to move the load.
In figure 1.8(b), we have an overview of possible types of EMA: first division in linear or rotary actuation unit, always depending on the application, and than geared or direct drive for the linear group; systems that require high torque must be equipped with a reduction gear, in order to adapt the motor features without the necessity to have an extremely performant one; instead if the load conditions are not extremely heavy and the motor characteristics are sufficient for the application, it is possible to use a direct connection between them.
For any kind of actuator, depending on the application, is generally important to have a control strategy: this is usually done using sensors(velocity and position) that by means of a closed loop strategy, is able to control the motor properly for the necessities, as shown in figure 1.9.
The design phase of an EMA, and in general of a mechatronic system, can be regulated by some concepts of design methodology useful to have guidelines from the preliminary steps up to the end of the process.
An example known in literature, as stated in [3], is the concept of the V shape design for mechatronic systems, like in figure 1.10; the starting point is always the need, or to be more precise, the targets of the system; these are in general defined by the customer that, through specifications and standards, make them clear and accessible by the manufacturer.

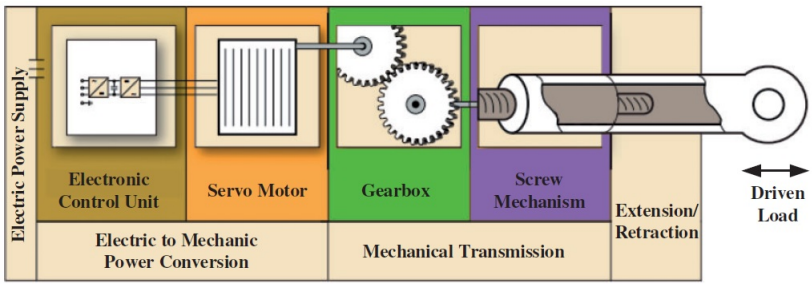

(a)

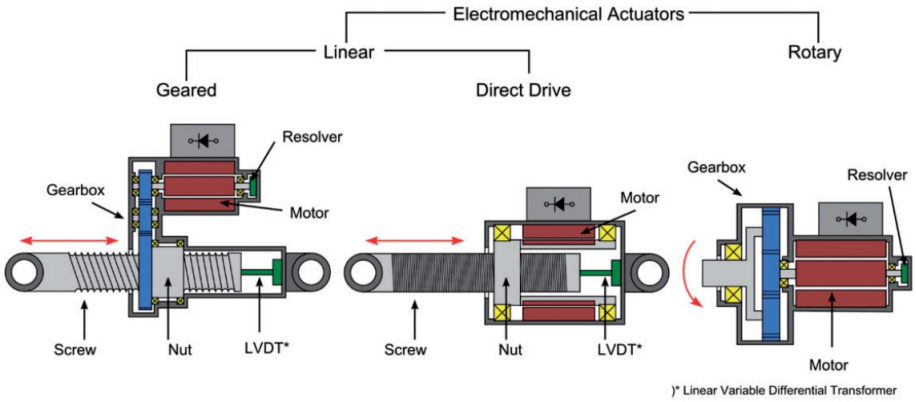

(b)

Figure 1.8: a)EMA general configuration and b)EMA typologies

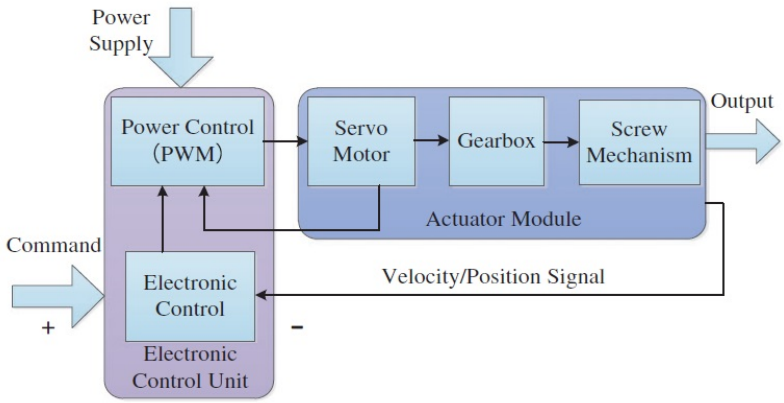

Figure 1.9: Closed loop strategy functional diagram

Passing through the architecture definition, components specification and different tests, we can conclude the process with the product definition: these steps are

part of a bigger stage, called prototyping.
In the preliminary design, phase that will be underlined in the work, it's important to have defined which are the design drivers [4], which are those parameters that have influence on the different components of our mechatronic system, like mechanical stress, geometric constraints, current draw and so on.

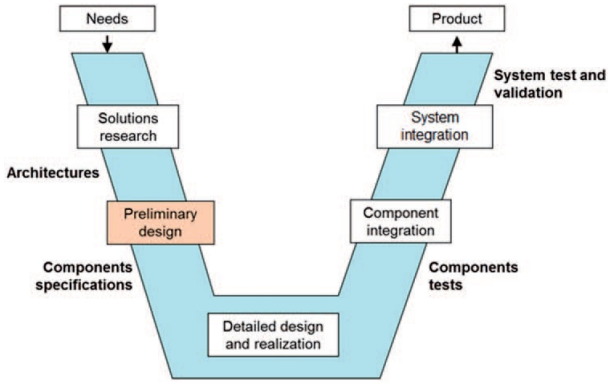

Figure 1.10: V-cycle design for a mechatronic system

Fundamental in this type of design is to understand properly the connection that links electric motors, command electronics, control techniques and machine mechanics: this is perfectly explained in [5], reference that will be used in the next sections for different purpose to achieve the desired actuator design.

1.3 Thesis organization

After this brief introduction about actuators the final section is dedicated just to underline which will be the organization and targets of the thesis work:

1. Actuator study and design methodology
2. Basic simulations and tests
3. Possible improvements

1.3.1 Actuator study and design methodology

In the first phase, will be presented the current configuration of an actuator already realized by the company, and will be underlined which are the requirements for which the actuator must be designed, according to a customer specification.
Then, the system will be analyzed to verify it dynamically and statically, to observe the perfomances and to check whether the requirements are met or not. One of the most important task in this phase is the load study in order to be able to select and manage correctly the load and motor coupling.
After a first verification of the current system, will be explained the methodology for all the sizing phase of all the components present in the actuator.

1.3.2 Basic simulations and tests

In the second phase, using simulink and simscape, will be presented some basic simulation for the selected motor and load couplings, which are useful to make a first estimation of motor performance in relation to the load, and also an evaluatation as regards an important factor as the current draws
In addition, an actual test for the actuator's emergency function will be shown: thanks to the testing department of the Silatech, this activity has been carried out.

1.3.3 Possible improvements

The work that must be done for a whole system design like the one that will be presented, is a lot: for the aspects not studied in depth in the central chapters of the thesis, the last section tries to collect them in order to have an overview on all the aspects that require attention during the design. There will be an evaluation on what could be some possible betterments to make the system more reliable, performing in a better way.

Chapter 2

Actuator study

2.1 Customer specification

The customer request is about an eletromechanical actuator that is able to move the parking lock for a shift by wire transmission. The positions that the actuator must be able to select are just two: P and not P.
The parking lock is engaged mechanically in the transmission by means of a selector cable between the actuator and the transmission parking lock shaft.
First of all we can identify the 3 main systems that are requested:

- main actuation unit
- parking emergency safety function unit
- transmission emergency actuation unit

2.1.1 Main actuation unit

For the main actuation unit, the specific requirements are:

- total travel distance: 12.5 mm
- necessity to actuate both pushing and pulling forces
- force to disengage the parking lock: 500 N(worst case, max weight and 30% slope)
- force to engage the parking lock: 200 N(worst case)
- max actuation time in worst load condition: 700 ms
- weight target: <1400 g
- maximum size of the entire system: 124 x 296 x 49.4 mm

In addition, there are also limitations in terms of current draw, which are summarized in table 2.1.

Designation	**Value**
Sleep mode (quiescent current)	$100\,[\mu A]\,Max$
Work mode (operating current)	$30000\,[mA]\,Max$
Work mode (typical operating current)	$5000\,[mA]$

Table 2.1: Limitations on current draws

It's important to underline that the load of 500 N, that is the worst case situation, is not a constant load: can be considered a dynamic load because, like represented in 1.7, after few mm of travel the load decreases, doesn't remain constant along the travel.

2.1.2 P emergency safety function unit

Nowadays, safety comes first in every type of field of application: here the request is about an emergency unit, the P emergency safety function unit: it is necessary because is required that, in case of a fault, the parking lock in the transmission is automatically engaged, without external energy supply (e.g. in the event of the loss of power supply).
In the transmission, the parking lock is engaged only when the vehicle speed falls below a defined limiting speed, so the system must be equipped with a mechanical energy storage device that can engage the P driving mode at any time.
In addition, this energy storage device must be kept in the charged state by an electromagnetic system (e.g. retaining magnet).

2.1.3 Transmission emergency actuation unit

In the event of a malfunction, to enable the disengage of the P position, a purely mechanical disengaging of the P driving mode must be provided by means of the actuator.
This kind of operation must be possible from inside the vehicle: generally this operation is realized using a specific tool, like a key, in order to avoid involuntary activations.
This actuation unit study is not the core topic of this thesis , but a preliminary analysis will be reported in the possible improvements chapter.

2.2 Actuator: case of study

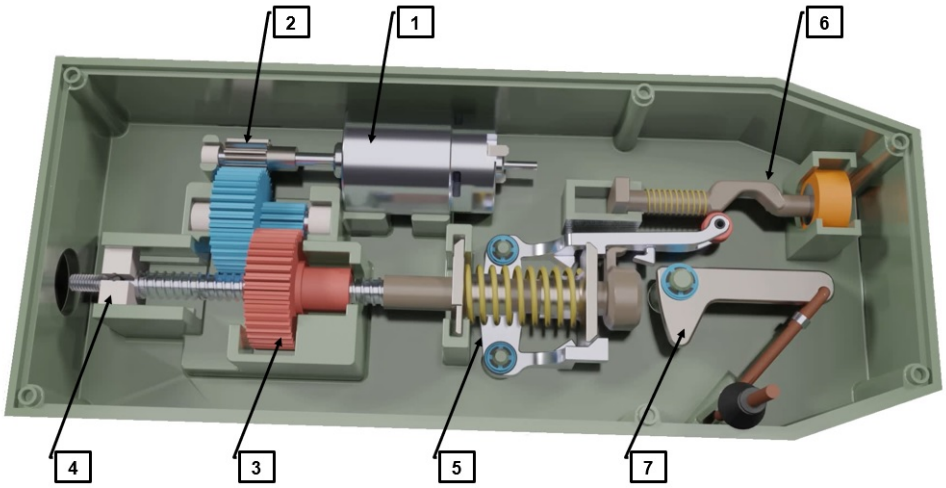

Figure 2.1: Rendered image of the realized actuator

As described in the introduction, the study starts with the analysis of an already realized system.
It is possible to observe,in figure 2.1, the solution elaborated by the company:

1) dc motor;

2) transmission: the reduction system in this kind of application is necessary to have sufficient torque to win the load;

3) leadscrew mechanism: to have transformation of the motion from rotational to translational, it is used this mechanism, with rotation of the last gear and screw translation; the last gear is directly part of the nut;

4) hall position sensor: to have precise motions, the motor needs a closed loop control

5) P safety system: when it is free to move, the compressed spring is able to pull the screw to the right, inserting the P position; all the right part of the actuator is related to the safety functions;

6) unlocking system: when there isn't current, the orange electromagnet release the system, and P emergency function is enabled;

7) manual lever: rotating lever to remove the P position in case of power supply loss; transmission emergency actuation unit;

Normal operation

During normal operation, only the left side of the actuation system and the screw are moved: the pull force is exerted by a motion of the screw to the right, looking to the previous image, and this motion engages the parking lock; instead, the push force is exerted by a motion of the screw to the left, and this motion disengages the parkin lock.

Emergency operation

In case of a malfunction, the actuation unit must be able to engage the parking lock without using directly the electric motor.
The idea developed by the company was to use a spring coaxial to the screw able to pull the cable and move it for the necessary travel: in figure 2.2, in case of a power supply failure, the electromagnet stops to retain the lateral rod in brown (figure refemergfigure) and the mechanical crab, in grey, is free to release the spring. in the image, it is represented the situation with the emergency system released.

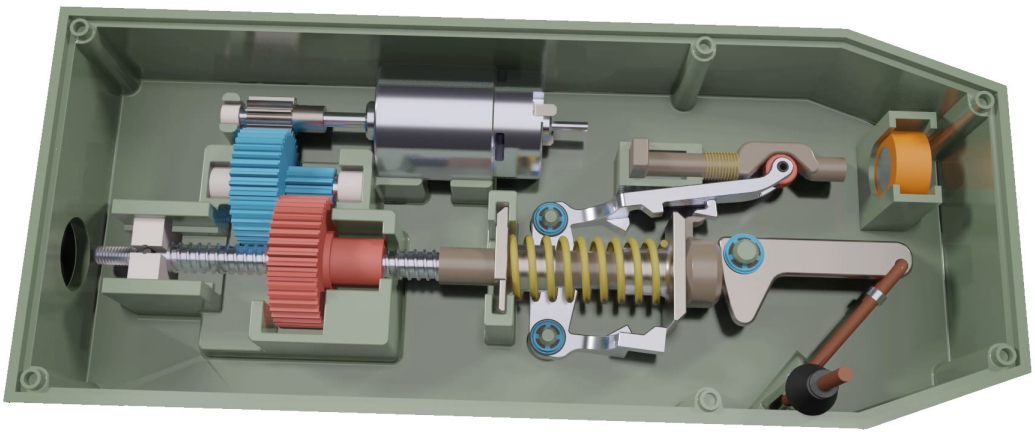

Figure 2.2: Emergency actuation unit activated and mechanical spring released

Manual operation

In case of a malfunction, if the car remains with the parking lock engaged without power supply, an operator must be able to disengage the lock manually in order to move the car. This is realized by means of a manual lever connected to a rope or a cable that can be pulled from inside the cabin. In figure 2.3, it is represented this condition.

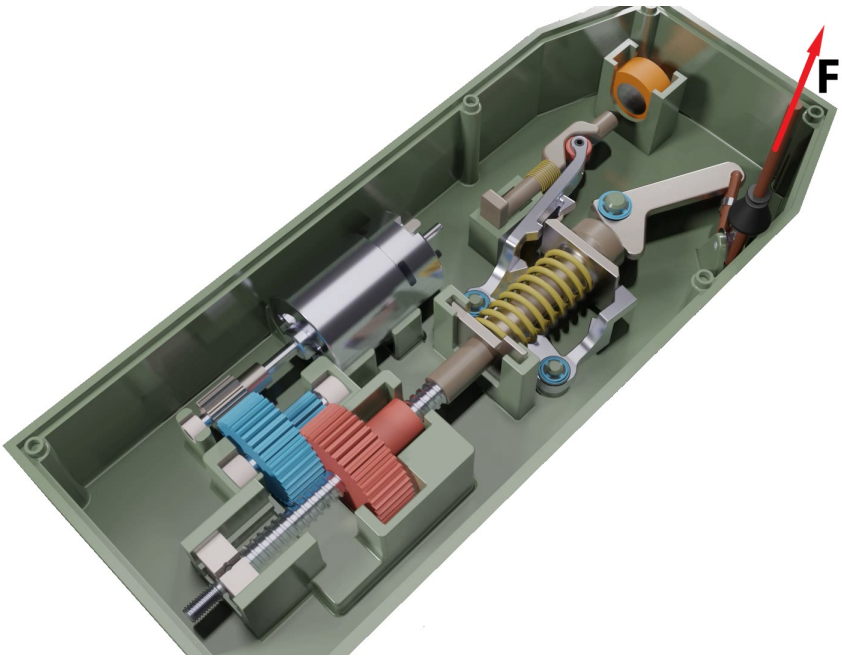

Figure 2.3: Transmission emergency actuation unit activation and force application

Motor and transmission system

The system composed by dc motor and reduction gear is a carry over part from an older project for which the targets were different, so first of all we have to summarize what are the data from which the analysis has started:

- **dc brushed motor**:

model	Maxon DCX 32L	**stall torque**	1730 mNm
nominal V	12	**stall current**	111 A
nominal speed	6560 rpm	**max efficiency**	85%
nominal torque	89.4 mNm	**rotor inertia**	77.6 gcm^2
nominal current	6 A	**no load speed**	7120 rpm

Table 2.2: Initial selected motor features

- **reduction gear**:

gear 1	$Z_1 = 15$, $m_1 = 0.011$ Kg	**gear ratio**	6.67
gear 2	$Z_2 = 30$, $m_2 = 0.017$ Kg	**material**	plastic
gear 3	$Z_3 = 15$, $m_3 = 0.011$ Kg	**efficiency**	0.91
gear 4	$Z_4 = 50$, $m_4 = 0.026$ Kg	**gears module**	1

Table 2.3: Current reduction gear features

The efficiency of the system has been computed as follows:

$$\begin{aligned} \eta_{i,j} &= 1 - \frac{1}{2}\left(\frac{1}{Z_i} + \frac{1}{Z_j}\right) \\ \eta_{tot} &= \eta_{1,2} \cdot \eta_{3,4} = 0.95 \cdot 0.96 = 0.91 \end{aligned} \tag{2.1}$$

- **leadscrew and nut mechanism**:

Leadscrew		**Nut**	
diameter	10 mm	**inner diameter**	10 mm
pitch	12 mm	**pitch**	12 mm
material	steel	**material**	iglidur j
$\boldsymbol{\eta_d}$, $\boldsymbol{\eta_r}$	0.64,0.52		
friction coeff $\boldsymbol{\mu_s}$	0.175		
thread angle	21.54°		

Table 2.4: Current leadscrew and nut mechanism features

The friction coefficient is considered for relative motion between steel and iglidur J (an Igus plastic material[6]).
The efficiency calculation and the system specification will be underlined in the next sections.

In the next section, the current actuator configuration will be studied in deep and will be clarified the features of the components, in order to verify the effectivenes of the selected solutions and, in addition, to highlight the methodology generally used for the actuators design.

2.2.1 Motor-load coupling

The study of the motor and load coupling is extremely important in a system in which we have an electric motor and a load to move: this analysis is useful to solve different practical problems like transients motions, optimal reduction ratio, verification for motor and gearbox, selection of motor size, as perfectly explained in [5].
First of all it is important to define which is the mechanical characteristic of a motor, that expresses the relation between torque and speed in a graph $C_m - \omega_m$, like in figure 2.4. Generally, working on the voltage value V, the characteristic can be translated upward or downward: the area between the line and the axes defines all the possible working points for the motor.
In this area, we can identify a division: a zone with continuous operating conditions and a zone with intermittent operating conditions. These zone are really important in relation to the load because, if we work for a long time in the intermittent zone, the risk is to overheat the motor or ,worse, to damage it irreversibly.

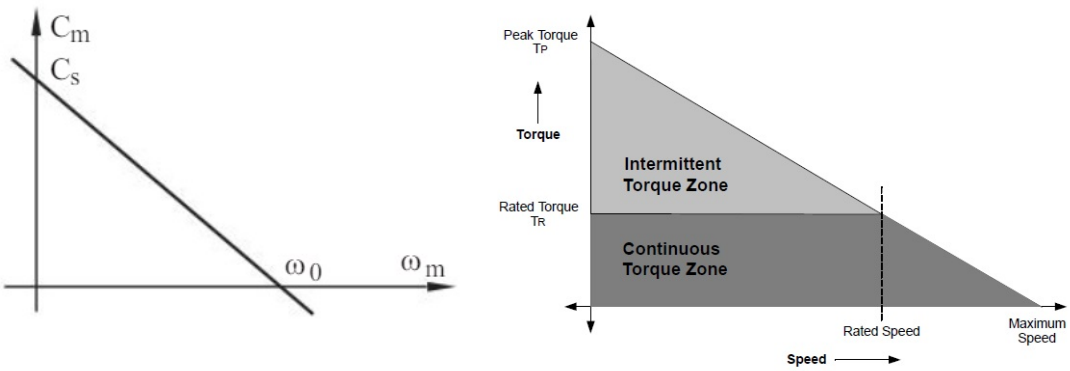

Figure 2.4: Dc motor mechanical characteristic (on the left) and operating zones (on the right)

The same characteristic can be defined for the load in a $C_r - \omega_r$ graph: this change in relation to the load type.
As already stated, generally it is not possible or convenient to use a direct connection between the motor and the load, and in that condition, like in this project, is suitable to interpose a reduction to adapt the motor torque to the load one.
The transmission ratio is defined as:

$$\tau = \frac{\omega_2}{\omega_1} \tag{2.2}$$

The use of a reduction gear introduces possible losses due to friction, so we have to take into account the efficiency to be able to know how much torque we are

delivering to the output shaft. We can define direct or retrograde efficiency:

$$\eta_d = \frac{C_2\omega_2}{C_1\omega_1} \qquad \eta_r = \frac{C_1\omega_1}{C_2\omega_2} \tag{2.3}$$

To take into account the dynamics of the system, it is important to define the dynamic equilibrium equations suitably reduced to the drive shaft or to the driven shaft:

$$C_m - \tau C_r = \left(J_m + \tau^2 J_r\right)\frac{d\omega_m}{dt} \tag{2.4}$$

$$\frac{C_m}{\tau} - C_r = \left(\frac{J_m}{\tau^2} + J_r\right)\frac{d\omega_r}{dt} \tag{2.5}$$

Determination of τ_{opt}

The selection of the right τ is not an easy task and has a great influence on the effectiveness of the system. Considering initially the transients, so more focus on the acceleration $\frac{d\omega_r}{dt}$, we can analyze two condition; starting with $C_r = 0$ (pure inertial load):

$$\frac{d\omega_r}{dt} = \frac{C_m}{\frac{J_m}{\tau} + \tau J_r} \tag{2.6}$$

The value of the optimal τ is a value for which we have the greatest acceleration of the load, and looking to the equation 2.6, this is obtained making smaller the denominator of the second member:

$$\frac{d}{d\tau}\left(\frac{J_m}{\tau} + \tau J_r\right) = 0 \tag{2.7}$$

$$-\frac{J_m}{\tau^2} + J_r = 0 \tag{2.8}$$

$$\tau = \tau_{opt} = \sqrt{\frac{J_m}{J_r}} \tag{2.9}$$

In figure 2.5, it is possible to see how the load space is modified in relation to the τ value.
Instead, considering $C_r \neq 0$ we have again the expression of the equation 2.6 for C_m and the expression of τ_{opt} changes:

$$\tau_{opt} = \sqrt{\frac{J_m\dot{\omega}_r}{J_r\dot{\omega}_r + C_r}} \tag{2.10}$$

Furthermore, we have to consider also the speed for which we have a minimum value of τ, that is a kinematic constrain:

$$\frac{\omega_{r,max}}{\tau} \leq \omega_{m,max} \quad \Longrightarrow \quad \tau \geqslant \frac{\omega_{r,max}}{\omega_{m,max}} = \tau_{min,kin} \tag{2.11}$$

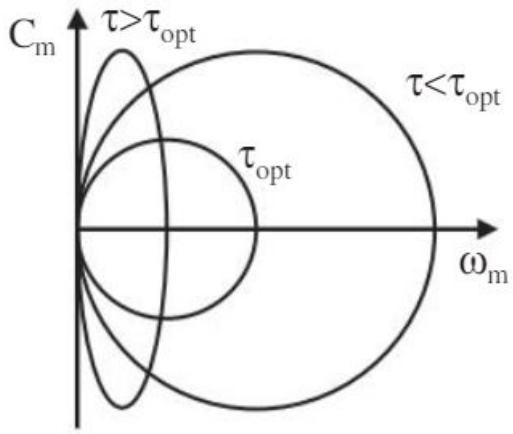

Figure 2.5: Effect of τ on the load space

Instead the maximum value of τ is related to the torques:

$$C_{m,max} > \tau C_{r,max} \quad \Longrightarrow \quad \tau \leq \frac{C_{m,max}}{C_{r,max}} = \tau_{max} \tag{2.12}$$

These considerations have to be specified for a condition in which the load is a generic dynamic load: in this case the determination of the optimum gear ratio is based on another important quantity, the root mean square motor torque $C_{m,rms}$. This quantity is important because when a motor works and produces torque, it also generates heat, that is the reason why the motor characteristic is divided in continuous and intermittent working zone. The $C_{m,rms}$ is used to determine the torque that is continuously substainable by the motor without damages and excessive heat generation:

$$C_{m,rms}^2 = \frac{J_m^2}{\tau^2}\dot{\omega}_{r,rms}^2 + \tau^2 \bar{C}_{rms}^2 + 2J_m(\dot{\omega}_r \bar{C})_{avg} \tag{2.13}$$

where $\bar{C}$ represents the istantaneous torque component that depends only on the load characteristic and reduction gear efficiency. Deriving this equation with respect to τ we obtain the optimum value:

$$\tau_{opt}^2 = \frac{J_m \dot{\omega}_{r,rms}}{\bar{C}_{rms}} \tag{2.14}$$

Generally it is really difficult to use the optimum value, so it is possible to determine a range of possible values using again the equation 2.13:

$$\tau_{max,min}^2 = \frac{-\tilde{B} \pm \sqrt{\tilde{B}^2 - 4\tilde{A}\tilde{C}}}{2\tilde{A}} \tag{2.15}$$

and the specific coefficient expressions are:

$$\tilde{A} = \bar{C}_{rms}^2 \qquad \tilde{B} = 2J_m(\dot{\omega}_r \bar{C}_{avg}) - C_n^2 \qquad \tilde{C} = J_m^2 \dot{\omega}_{r,rms}^2 \tag{2.16}$$

2.2.2 Motor and τ selection method for dynamic loads: cases of study

The load characteristic has not been explicitly provided in the customer specification, but cannot be considered as a constant load: as stated previously, the load will be considered as dynamic. In addition, the system, working for a small amount of time, will never reach regime conditions.
The general procedure for the selection is composed of these steps:

1) motion law choice, if not directly provided
2) first selection considering root mean square torque (C_{rms})
3) verification of constraints and eventually return to previous steps

Instead, the general checks that must be satisfied, as expressed also in [7], are:

- instantaneous maximum torque (peak torque verification): $C_{max} < C_{m,max}$
- root mean square torque (thermal verification): $C_{m,rms} < C_{nom}$
- maximum velocity: $\omega_{max} < \omega_{m,max}$

1) Case study: worst load condition in normal operation

To start with the calculation, we need some data. For simplicity, it is better to have the load characteristics calculated with respect to the nut on the leadscrew mechanism, in order to have just rotational quantities and not rotational and translational together. So starting from the geometrical features of the leadscrew mechanism, we can compute his efficiency by means of the equivalent edges, like in figure 2.6,[8] :

$$\Delta z = \Delta x \tan \alpha \tag{2.17}$$

in which Δz is the vertical translation in the figure, Δx is the horizontal one and α is the thread inclination. Δx is function of the rotation of the screw $\Delta\theta$:

$$\Delta x = \frac{d}{2}\Delta\theta \tag{2.18}$$

than we can write the equilibrium for vertical and horizontal translations:

$$\begin{aligned} P &= F\cos(\phi + \alpha) \\ T &= P\tan(\phi + \alpha) \end{aligned} \tag{2.19}$$

ϕ is the friction angle, calculated using the average friction coefficient of the material taken from Igus catalogue [6] $f_{static} = 0.175$:

$$\phi = \tan^{-1} f_{static} = 9.92° \tag{2.20}$$

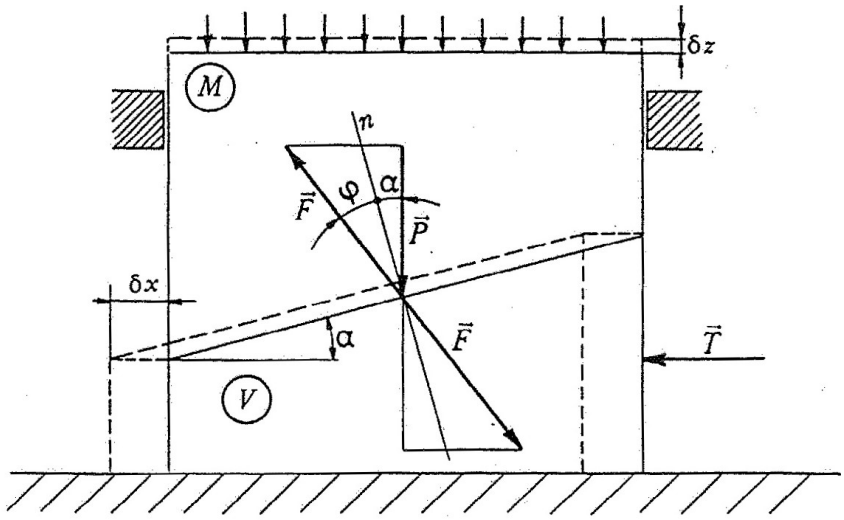

Figure 2.6: Equivalent wedges for leadscrew and nut mechanism

Taking into account the torque applied to the nut:

$$M_n = T\frac{d}{2} \tag{2.21}$$

the efficiency becomes:

$$\eta_d = \frac{P_o}{P_i} = \frac{P\Delta z}{M_n \Delta\theta} = \frac{\tan\alpha}{\tan(\phi+\alpha)} = 0.65 \tag{2.22}$$

Considering the worst case of 500 N, we can compute the torque acting on the last gear considering the leadscrew and nut mechanism [9]:

$$C_r = \frac{FP}{2\pi\eta_d 1000} = \frac{500\cdot 12}{2\pi\cdot 0.65\cdot 1000} = 1.51 \quad [Nm] \tag{2.23}$$

This kind of resistant torque doesn't include the efficiency of components in motion with the screw, like bearings and other transmission parts, so this value has to be increased of about 10%:

$$C_r = 1.51\cdot 1.1 \approx 1.66 \tag{2.24}$$

The load inertia, considered from the nut point of view, can be computed as:

$$J_r = R^2 M_{transl} = 0.0019^2\cdot 0.1 = 3.64\cdot 10^{-7} \quad [Kgm^2] \tag{2.25}$$

in which R is called transformation ratio of the lead screw mechanism, defined as:

$$R = \frac{v}{\omega} = \frac{pitch}{2\pi} = \frac{12\cdot 10^{-3}}{2\pi} = 0.0019 \quad [m/rad] \tag{2.26}$$

and M_{transl} the translating mass, for which we have we consider all the parts attached to the screw, so a quantity of 0.1 Kg.
More details about leadscrew and nuy mechanism will be given in the next sections.
Now we need to define the motion law, a suitable initial solution to start with the calculation: there are different possible solutions of motion laws, like cicloidal, with piecewise constant acceleration or polynomial.
The trajectory planning it is studied in deep in [10]. Using the second option, we have the graphs represented in the next page, in figure 2.7. The max speed is calculated knowing that the area under the speed diagram is equal to the travel:

$$V_{max} = \frac{2\Delta s_{lin}}{t_1 + t_2} = \frac{2 \cdot 12.5}{0.35 + 0.35} = 50 \cdot 10^{-3} \quad [m/s] \tag{2.27}$$

Considering 700 ms of available time for the travel, the time steps are the same between each other:

$$t_1 = t_2 = \frac{0.7}{2} = 0.35 \quad [s] \tag{2.28}$$

Now we have to define which is the maximum angular speed of the nut, so we need first of all the total rotation of the nut in relation to the 12.5 mm of linear travel:

$$\Delta S_{ang} = \frac{R}{\Delta s_{lin}} = \frac{0.0019}{12.5} = 6.54 \quad [rad] \tag{2.29}$$

and using this quantity we can compute the angular speed:

$$\begin{aligned} \Delta S_{ang} &= \omega_{r,max}\left(\frac{t_1 + t_2}{2}\right) \\ \omega_{r,max} &= \frac{2\Delta S_{ang}}{t_1 + t_2} = \frac{2 \cdot 6.54}{0.7} = 18.7 \quad [rad/s] \end{aligned} \tag{2.30}$$

With the value of the angular speed, it is possible to compute the maximum acceleration for the two sections of the graph:

$$\dot{\omega}_{r,max} = \frac{\omega_r}{t_1} = 53.43 \quad [rad/s^2] \tag{2.31}$$

An initial motor selection is done using two characteristic factors: as explained in [7], we have two parameters, one that characterized the motor, that is α, and one that caracterized the load, that is β. They are defined as:

$$\alpha = \frac{C_n}{\sqrt{J_m + J_{rid}}} \tag{2.32}$$

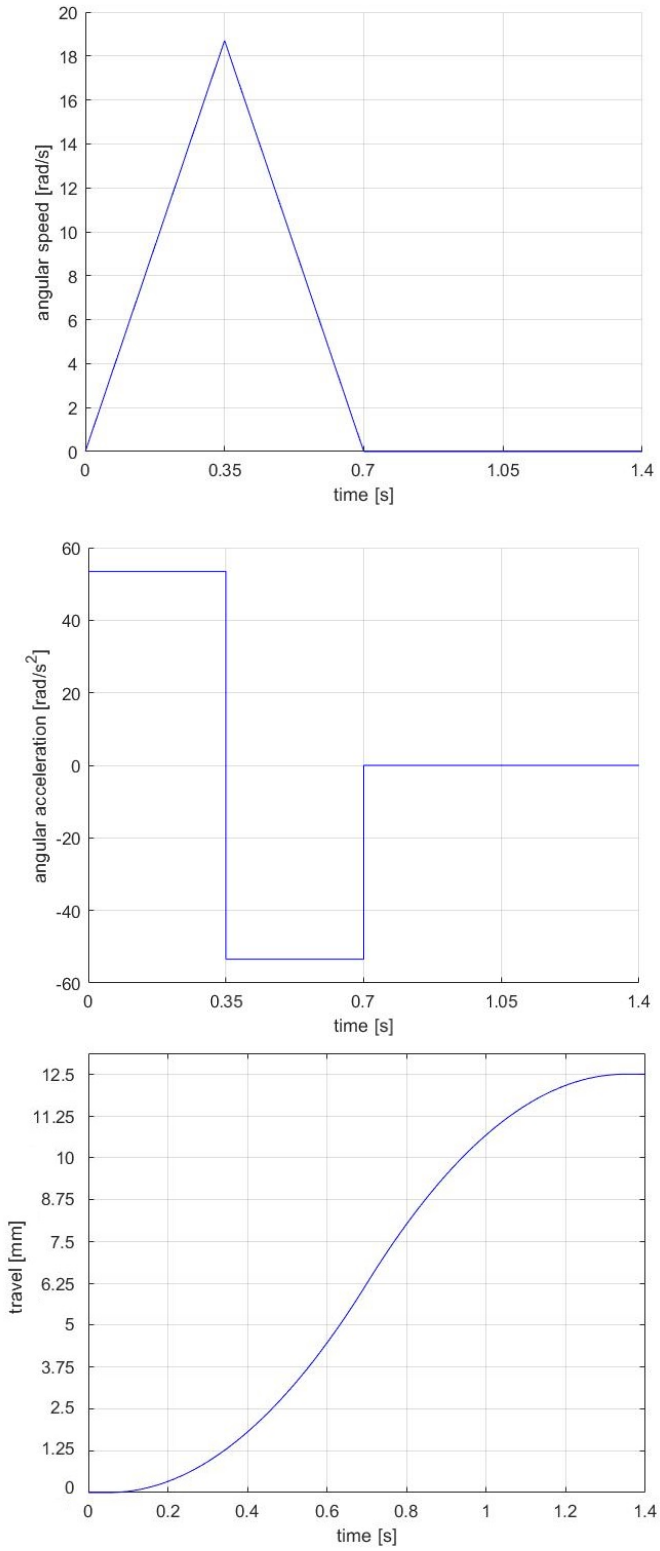

Figure 2.7: From the top: speed profile, acceleration profile, travel profile

in which C_n is the nominal torque of the motor, J_m is the rotor inertia and J_{rid} is the gear reductor inertia. Instead for β:

$$\beta = \sqrt{2}\sqrt{\dot{\omega}_{r,rms}\bar{C}_{rms} + (\dot{\omega}\bar{C})_{avg}} \tag{2.33}$$

Now we define the motor torque at the last gear in the two intervals of the motion law graph. It is important to underline that the resistant torque given by the load, is high in the first few millimeter, and than decreases quite vertically in the travel, so after few ms of motion the remaining load is given by the cable dragging.

The cable dragging force has been evaluated by some examples given by the Silatech Srl, that has also a testing lab: the highest force noticed in all the tests was close to 10 N, so considering that force the resistant torque on the last gear is calculated as in the equation 2.23:

$$C_{r2} = \frac{10 \cdot 12}{2\pi \cdot 0.65 \cdot 1000} = 0.0029 \quad [Nm] \tag{2.34}$$

For simplicity we start with direct efficiency of the gears $\eta_d = 0.9$ and retrograde $\eta_r = 0.8$:

$$\begin{aligned} \bar{C}_1 &= \frac{J_r\dot{\omega}_{r1} + C_{r1}}{\eta_d} = \frac{3.64 \cdot 10^{-7} \cdot 53.43 + 1.66}{0.9} = 1.83 \quad [Nm] \\ \bar{C}_2 &= (J_r\dot{\omega}_{r3} + C_{r3})\eta_r \\ &= [3.64 \cdot 10^{-7} \cdot (-53.43) + 0.0029] \cdot 0.8 = -0.027 \quad [Nm] \end{aligned} \tag{2.35}$$

Coming back to the equation 2.33, we can compute the coefficients. The total cycle time T has to take into account also a pause time after the motion, defined as *Dwell time*: this value has influence on the C_{rms}, reducing it. In the next pages will be figure out this effect.
Now, for the initial computations, we consider a *Dwell time* of 0.7s, that means to use the 50% of the total time for the actual motion:

$$\bar{C}_{rms} = \sqrt{\frac{\sum \bar{C}_i^2 t_i}{\sum t_i}} = \sqrt{\frac{1.83^2 \cdot 0.35 + (-0.02)^2 \cdot 0.35}{1.4}} = 0.91 \quad [Nm] \tag{2.36}$$

$$(\dot{\omega}\bar{C})_{avg} = \frac{\sum \dot{\omega}_i \bar{C}_i t_i}{\sum t_i} = \frac{53.43 \cdot 1.83 \cdot 0.35 - 53.43 \cdot (-0.02) \cdot 0.35}{1.4} = 24.77 \tag{2.37}$$

$$\dot{\omega}_{r,rms} = \sqrt{\frac{\sum \dot{\omega}_i^2 t_i}{\sum t_i}} = \sqrt{\frac{2 \cdot 53.43^2 \cdot 0.35}{1.4}} = 37.78 \quad [rad/s^2] \tag{2.38}$$

Knowing all the coefficients it's possible to calculate β:

$$\begin{aligned} \beta &= \sqrt{2}\sqrt{\dot{\omega}_{r,rms}\bar{C}_{rms} + (\dot{\omega}\bar{C})_{avg}} \\ &= \sqrt{2}\sqrt{37.78 \cdot 0.91 + 24.77} = 10.89 \end{aligned} \tag{2.39}$$

This value must be compared with α for the motor selection:

$$\alpha \geq \beta \tag{2.40}$$

and if this inequality is satisfied, this is a first step to select the suitable motor.
For a precise calculation of the α value, at the denominator is also present the value of the gear reductor inertia.
This component has not been selected yet, so we start from the value of the current gear reductor as a starting point: this quantity has to be transposed up to the drive shaft using the transmission ratio using Lagrange equation, as explained properly in [11].
With the kinetic energy equation, we can compute the equivalent inertia of the gear reductor moved to the drive shaft:

$$\begin{aligned} T &= \frac{1}{2}\sum(I_i\tau_i^2)\omega_m = \frac{1}{2}I_{eq}\omega_m^2 \\ I_{eq} &= \sum I_i\tau_i^2 \\ &= I_1 + \frac{I_2\tau_{12}^2}{\eta_{12}} + \frac{I_3\tau_{13}^2}{\eta_{13}} + \frac{I_4\tau_{14}^2}{\eta_{14}} = 1.32 \cdot 10^{-6} \quad [Kgm^2] \end{aligned} \tag{2.41}$$

The specific mass moment of inertia of each gear has been calculated as:

$$I_i = \frac{1}{2}m \cdot r^2 \tag{2.42}$$

with r considered as gear external radius. In table 2.3 has been reported dimensions and masses of each gear.
The α value becomes:

$$\alpha = \frac{C_n}{\sqrt{J_m + J_{rid}}} = \frac{0.09}{7.76 \cdot 10^{-6} \cdot 1.24 \cdot 10^{-6}} = 29.67 \tag{2.43}$$

so the equation 2.40 is respected.
Now the next step is the selection of the gear reductor, so we can use the equations 2.15 and 2.16 for the calculation of the range values:

$$\begin{aligned} \tilde{A} &= 0.84 \\ \tilde{B} &= -0.01 \\ \tilde{C} &= 8.59 \cdot 10^{-8} \end{aligned} \tag{2.44}$$

so:

$$\tau_{max,dyn} = 0.09 = \frac{1}{10.53} \qquad \tau_{min,dyn} = 0.03 = \frac{1}{296.05} \tag{2.45}$$

and the value of τ_{opt} using equation 2.14:

$$\tau_{opt}^2 = \sqrt{\frac{J_m\dot{\omega}_{rms}}{\bar{C}_{rms}}} = 0.02 = \frac{1}{55.84} \tag{2.46}$$

Instead, the kinematic constraint on the gear ratio is:

$$\tau_{min,kin} = \frac{\omega_{r,max}}{\omega_{m,max}} = 0.025 = \frac{1}{39.87} \tag{2.47}$$

The gear ratio that was selected initially was $\tau = 0.15$ (i=6.67): it is clear that, at least for the continuous operating conditions, the selected gear ratio is not sufficient to guarantee a safe operation of the motor.
Now we can select a possible value of the gear ratio in that range and verify the point of continuous working and of peak torque.
For the continuous operating point, we need to compute the $C_{m,rms}$ from equation 2.13 but also considering the efficiencies:

$$C_{m,rms}^2 = \frac{J_m^2}{\tau^2}\dot{\omega}_{r,rms} + \tau^2\left(\frac{\bar{C}_r}{\eta}\right)_{rms}^2 + 2J_m\left(\frac{\dot{\omega}_r\bar{C}_r}{\eta}\right)_{avg} \tag{2.48}$$

It is clear that this value is influenced by the gear ratio.
Then to verify the working point of course we need the $\omega_{m,rms}$, that is defined as:

$$\begin{aligned}\omega_{r,rms} &= \sqrt{\frac{1}{T}\int_0^T \omega_r^2 dt} = \sqrt{\frac{1}{T}\int_0^{t_1}\left(\omega_{r,max}\frac{t}{t_1}\right)^2} \\ &= \omega_{r,max}\sqrt{\frac{t_1/3}{T}} = 18.7\sqrt{\frac{0.35/3}{0.35}} = 10.8 \quad [rad/s]\end{aligned} \tag{2.49}$$

so:

$$\omega_{m,rms} = \frac{\omega_{r,rms}}{\tau} \tag{2.50}$$

and we can summarize different possible values with different selections of τ, as shown in table 2.5.

i	$\boldsymbol{\tau}$	$\boldsymbol{\omega_{m,rms}}$**[rpm]**	$\boldsymbol{C_{m,rms}}$**[mNm]**
9	1/9	928	113.7
12.5	1/12.5	1289	83.1
13.5	1/13.5	1392	77.4
14.5	1/14.5	1495	72.5
15.5	1/15.5	1598	68.2
17.5	1/17.5	1804	61.3

Table 2.5: Rms values for different possible values of τ

To verify if the working point is suitable for the continuous working, we need to use the mechanical characteristic of the motor and verify that the point $(\omega_{m,rms}, C_{m,rms})$

is located in the continuous torque zone of the motor: as it is possible to see in figure 2.8, for a gear ratio smaller than the $\tau_{max,dyn}$, that is the

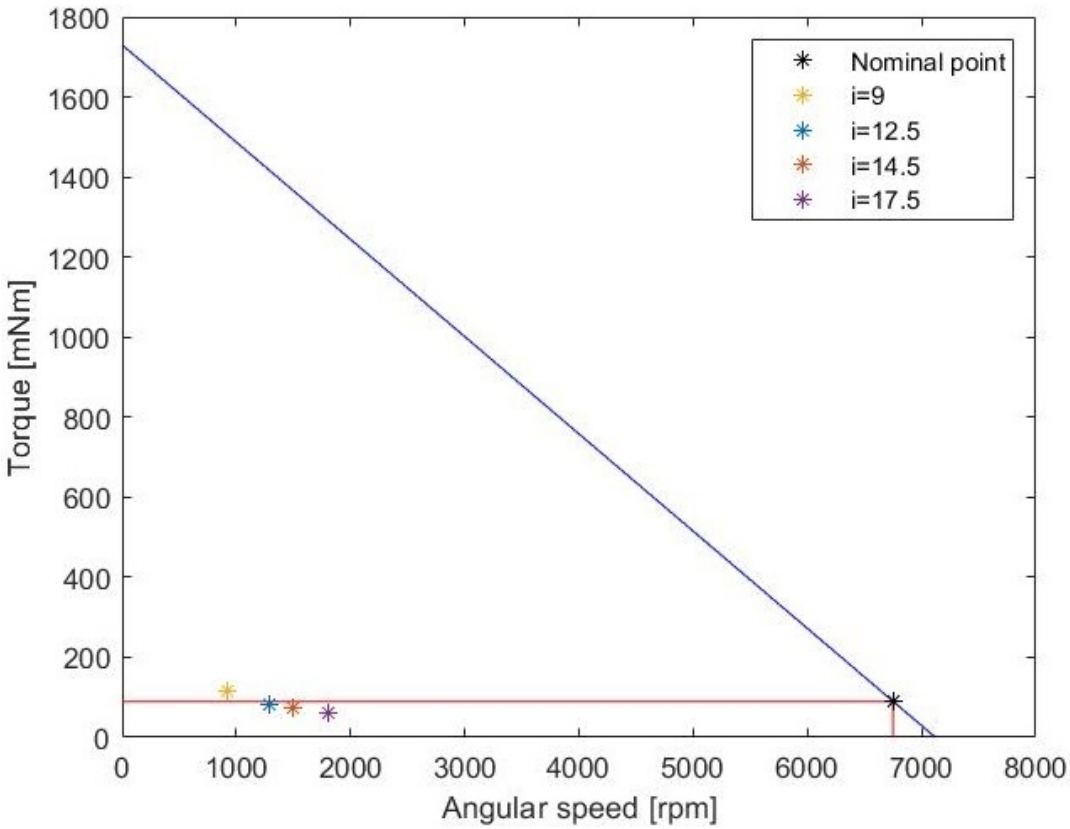

Figure 2.8: Maxon DCX 32L mechanical feature and rms points for different values of τ

point with i=9, the working point is above the continuous working zone of the motor and the selection of that gear ratio is not possible.
For the other values, the working point is inside the continuous zone, and those gear ratios can be used for the application.
For the peak torque, again we have to verify the working point, so we need to compute $\omega_{m,max}$ and $C_{m,max}$.
For the latter, we have to use again the equation 2.48 but with all the values referred not to rms but to the maximum quantities and in table 2.6 it is possible to summarize the results.

Same as before, we can plot in figure 2.9 those points on the mechanical feature of the motor to verify if the peak torque is smaller than the maximum available by the motor.

i	τ	$\omega_{m,max}$[rpm]	$C_{m,max}$[mNm]
9	1/9	1607	227.2
12.5	1/12.5	2232	166
13.5	1/13.5	2410	155
14.5	1/14.5	2590	144.6
15.5	1/15.5	2767	136
17.5	1/17.5	3125	122

Table 2.6: Rms values for different possible values of τ

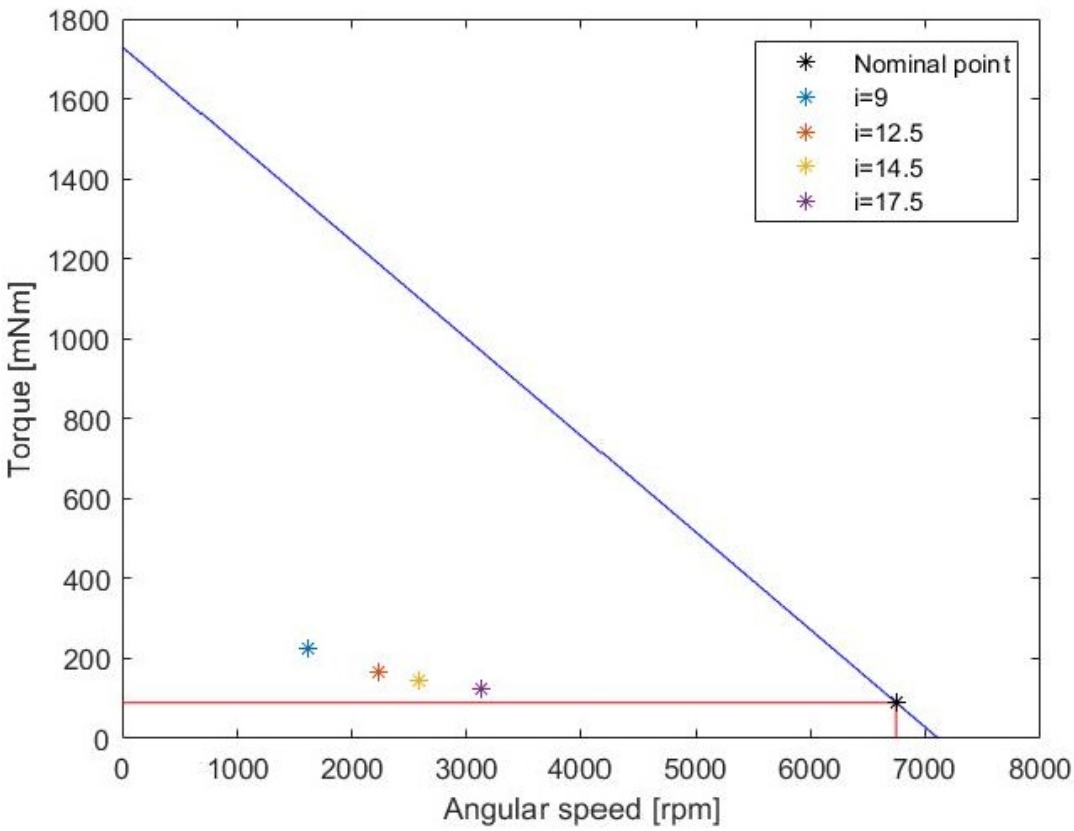

Figure 2.9: Maxon DCX 32L mechanical feature and peak points for different values of τ

As it is possible to figure out, this motor has a peak torque extremely high for the application, but the continuous torque looks quite appropriate.

Dwell time effect: as introduced previously, the total period of the motion law has to take into account also a pause time, in order to reduce all the rms quantities and reduce the possible overheating of the motor.
The computations are the same done previously considering a different time of pause, and in the table 2.7 it is possible to observe the differences: the "effective motion percentage" means the percentage of the whole period occupied by the actual motion.
It is possible to figure out how the quantities required by the load in terms of rms are affected by this pause time, and conseguently has effect on the required motor performances.
The actuator, being installed in a vehicle, in an actual use can have really small activation during a day: if we consider that the actuator should be used for the parking lock, we can estimate a use of maximum 10 times a day.
But in the designing phase, to validate the project, the system must be tested in order to simulate an entire vehicle life, to verify if the actuator is strong enough to substaine a durability test.
During a durability test, the cycle time is extremely reduced in order to test the system in a reasonable time: this must be considere for the definition of the *Dwell time*.

Effective motion percentage	**50%**	**35%**	**25%**
$\overline{C}_{rms}$ [mNm]	0.92	0.76	0.65
β load factor	10.9	9.11	7.70
τ max	0.09	0.11	0.14
τ min	0.0034	0.0028	0.0024
If τ= 0.07			
$C_{m,rms}$	0.075	0.063	0.053

Table 2.7: *Dwell* time effect

2) Case study: worst load condition in emergency operation

As stated initially, when the emergency unit is activated, a spring is released.
When the power supply return available, the actuation unit must be able to remove the parking lock: in that condition, the load is not anymore just related to the force needed to remove the lock, but in addition we have also the spring compression, as in figure 2.11.
In the first few millimeters of travel, the amount of load is 500 N, to remove the lock, and 56.7 N, for the spring preload, value that will be explained later.
The calculations made previosly, can be modified taking into account the different load condition in the two stages of the travel.
Later will be explained the spring force for which all the calculations have been made.

The torque that has to be applied at the last gear to win this load, can be computer as previously in equation 2.23:

$$C_r = \frac{FP}{2\pi\eta_d 1000} = \frac{556.7 \cdot 12}{2\pi \cdot 0.65 \cdot 1000} = 1.678 \quad [Nm] \tag{2.51}$$

Considering also here an increasing of 10%, the $C_r = 1.846 \quad [Nm]$.
Being an emergency operation, the frequency of possible activation of the system is much smaller than normal operation, so the *Dwell time* here can be further increased to reduce the effect of higher load condition: for this reason, is increased up to 1 second.
Avoiding to write again all the calculations, the computations are summarized in figure 2.10.
Same as before, in the table 2.8 and 2.9 are summarized the rms and peak values relative to different gear ratios.

Basic data					Root mean square values				
t1	0.35	s			ώr,rms	34.28	rad/s^2		
t2	0.35	s			Crms	0.98	Nm		
Dwell time	1	s			(ώC)average	30.57			
Ttot	1.70	s			β (load factor)	11.34			
t1+t2	0.70	s			α (motor factor)	29.67			
Travel	12.50	mm			Gear ratios				
Δs angular	6.54	rad	375	deg	A	0.96			
ωr max	18.70	rad/s			B	-0.01			
ώr,max	53.43	rad/s^2			C	0.00000007			
					τ opt	0.02	i opt	60.76	
Motor torque at the exit of the gear reductor					τ max	0.09	i max	11.40	
If F max=556.7	C1	2.03	Nm		τ min	0.00	i min	323.95	
	C2	-0.75	Nm		τ min, kin	0.03	i min, kin	39.87	

Figure 2.10: Emergency operation: calculations summary

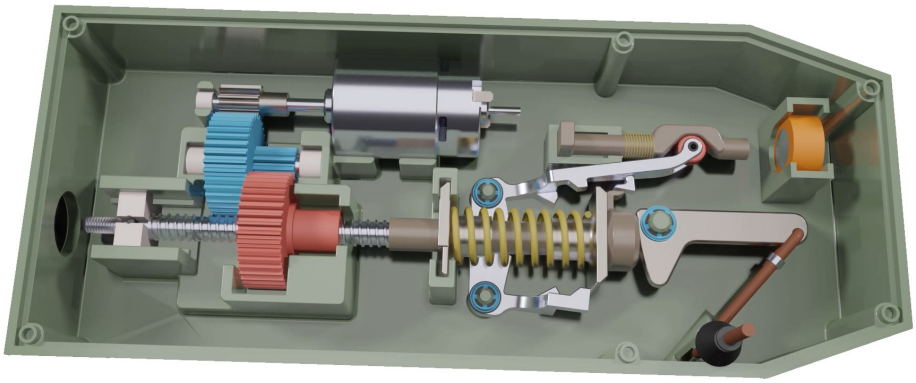

Figure 2.11: P Emergency actuation unit activated

i	τ	$\omega_{m,rms}$[rpm]	$C_{m,rms}$[mNm]
9	1/9	928	122.2
12.5	1/12.5	1289	89.5
13.5	1/13.5	1392	83.3
14.5	1/14.5	1495	78
15.5	1/15.5	1598	73.5
17.5	1/17.5	1804	66

Table 2.8: Emergency operation: rms values for different possible values of τ

i	τ	$\omega_{m,max}$[rpm]	$C_{m,max}$[mNm]
9	1/9	1607	252.02
12.5	1/12.5	2232	183.9
13.5	1/13.5	2410.7	171.06
14.5	1/14.5	2589.3	160.04
15.5	1/15.5	2767.9	150.49
17.5	1/17.5	3125	134.79

Table 2.9: Emergency operation: peak values for different possible values of τ

Now that we have an overview of the current system, is possible to make some considerations: first of all, the gear ratio that has been selected initially, was too small to guarantee a proper operation of the actuator, so must be chose a greater one; the motor is a really performant one, oversized for this application, so, in the next section, will be selected a motor and a gear ratio more suitable for the application.

2.2.3 Actual motor and τ selection

Consequently to the calculations previously made, is now possible to select the motor and the reduction gear: the selection of the reduction gear will be a trade off between the two load cases studied previously, considering that both will be worst conditions and not normal operations.
As seen before, the motor and reduction gear evaluation and selection are strictly related between each other.
One parameter that has not been taken into account for the motor selection is the current absorption in both normal and starting, or stall, conditions. This parameter is extremely influent on the motor selection.
The most important relations for a dc motor are the following:

- rotor flux: $\phi_r = k * i_a$
- drive torque: $T_m = K_t i_a$
- back efm: $e_{bmf} = K_e \omega_m$

where all the K are specific constants.
The basic scheme of a dc motor is represented 2.12.
From that scheme, using Kirchoff's law, it is possible to obtain the voltage:

$$V_a = e + Ri_a + L\frac{di_a}{dt} \tag{2.52}$$

If we want to consider and evaluate the stall current, we have to impose an $\omega_m = 0$ condition, for which from the previous equation $di_a/dt = 0$ and $e = 0$. So:

$$\begin{aligned} T_m &= K_t \frac{V_a}{R} \\ i_s &= \frac{V_a}{R} \end{aligned} \tag{2.53}$$

The stall current can be extremely higher with respect to the nominal one and in some conditions that high value is not substainable neither for a small period of time, if the motor is powered to the nominal voltage: there are control techniques to limit the starting current but they are not covered in this thesis work.
In the next page, in table 2.10, are summarized all the motor analyzed for the application with all the important features and the results.

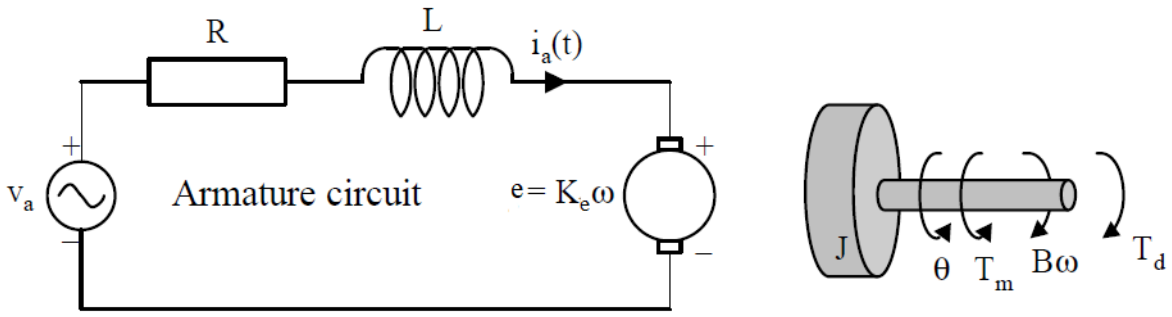

Figure 2.12: Dc motor electrical scheme

Worst case in normal operation	Maxon DCX26L	Maxon DCX32L	Maxon DCX35L	Maxon BLDC EC32	Maxon BLDC ECMAX30	Dunkermotoren BG32
Nominal Voltage [V]	12	12	12	12	12	12
Nominal Torque [mNm]	46.9	89.4	77.7	44.6	63.6	43.7
Nominal speed [rpm]	9460	6560	7610	13400	6590	4320
Rotor Inertia [gcm^-2]	21.4	77.6	99.5	20	21.9	10.2
Nominal current [A]	4.5	6	6	6.51	4.72	2.6
No load current [A]	131	274	320	662	302	274
No load speed [rpm]	10600	7120	8130	15100	7980	5560
Stall torque [mNm]	532	1730	2080	428	381	100
Stall current [A]	49.7	111	152	57.2	26.8	9
Dwell time [s]	0.70	0.70	0.70	0.70	0.70	0.70
β (load factor)	10.89	10.89	10.89	10.89	10.89	10.89
α (motor factor)	25.2	29.7	23.1	24.5	33.9	28.6
τ opt	0.0094	0.0179	0.0203	0.0091	0.0095	0.0065
τ max	0.0492	0.0950	0.0808	0.0467	0.0681	0.0463
τ min	0.0018	0.0034	0.0051	0.0018	0.0013	0.0009
τ min, cinematico	0.0168	0.0251	0.0220	0.0118	0.0224	0.0321
Worst case in emergency operation	**Maxon DCX26L**	**Maxon DCX32L**	**Maxon DCX35L**	**Maxon BLDC EC32**	**Maxon BLDC ECMAX30**	**Dunkermotoren BG32**
Nominal Voltage [V]	12	12	12	12	12	12
Nominal Torque [mNm]	46.9	89.4	77.7	44.6	63.6	43.7
Nominal speed [rpm]	9460	6560	7610	13400	6590	4320
Rotor Inertia [gcm^-2]	21.4	77.6	99.5	20	21.9	10.2
Nominal current [A]	4.5	6	6	6.51	4.72	2.6
No load current [A]	131	274	320	662	302	274
No load speed [rpm]	10600	7120	8130	15100	7980	5560
Stall torque [mNm]	532	1730	2080	428	381	100
Dwell time [s]	1	1	1	1	1	1
Stall current [A]	49.7	111	152	57.2	26.8	9
β (load factor)	11.80	11.80	11.80	11.80	11.80	11.80
α (motor factor)	25.2	29.7	23.1	24.5	33.9	28.6
τ opt	0.0086	0.0165	0.0186	0.0084	0.0087	0.0060
τ max	0.0454	0.0878	0.0743	0.0430	0.0630	0.0428
τ min	0.0016	0.0031	0.0047	0.0016	0.0012	0.0008
τ min, cinematico	0.0168	0.0251	0.0220	0.0118	0.0224	0.0321

Table 2.10: Dc motors analysis summary

On the basis of the data and the limitations given by the project, the motor that has been selected for the next analysis is the $Maxon\,Bldc\,Ecmax30$, that in terms of available torque and current absorption looks suitable for the application.
As already done for the first motor, also in this case we can analyze the behaviour in relation to the gear ratio.
Starting with the *rms* values, in the next table we can summarize the results considering both worst load conditions. With respect to a previous study, here we have different value of *Dwell time*, in particular they are greater for both normal and emergency operations: consciously increasing these times, it is possible to use a wider range of motors, while taking into account the actual motion time constraint of 0.7 seconds.

Worst load case in normal operation			D well time 1.3s
i	τ	$\omega_{m,rms}$[rpm]	$C_{m,rms}$ [mNm]
9	0.11	927.8	93.9
12.5	0.08	1288.7	67.9
13.5	0.074	1391.8	63
14.5	0.068	1494.9	58.8
15.5	0.064	1598.0	55.5
16	0.06	1649.6	53.3
17.5	0.057	1804.2	49
Worst load case in emergency operation			**D well time 1.8s**
i	τ	$\omega_{m,rms}$[rpm]	$C_{m,rms}$ [mNm]
9	0.11	927.8	99.5
12.5	0.08	1288.7	72
13.5	0.074	1391.8	66.8
14.5	0.068	1494.9	62.3
15.5	0.064	1598.0	58.4
16	0.06	1649.6	57
17.5	0.057	1804.2	51.9

Table 2.11: Rms values for $Maxon\,Bldc\,Ecmax30$ with different possible values of τ

Graphically we can plot, done just for the normal operations, some of the τ values on the mechanical feature of the motor, figure 2.13, and verify what gear ratio values are suitable in relation to the performances.
As it is possible to see, as before also here considering a τ value out of the range of permissible values, the nominal torque required to the motor $C_{m,rms}$ exceeds the nominal torque.
In table 2.12 same considerations for the peak values, and in the next page graphical representation of the results, figure 2.14, for normal operation.

Worst load case in normal operation			D well time 1.3s
i	τ	$\omega_{m,max}$[rpm]	$C_{m,max}$ [mNm]
9	0.11	1607	224.5
12.5	0.08	2232	162.3
13.5	0.074	2410	150.5
14.5	0.068	2590.3	140.4
15.5	0.064	2767	131.5
16	0.06	2857	130
17.5	0.057	3125	117
Worst load case in emergency operation			**D well time 1.8s**
i	τ	$\omega_{m,max}$[rpm]	$C_{m,max}$ [mNm]
9	0.11	1607	249.36
12.5	0.08	2232	180.24
13.5	0.074	2410	167.12
14.5	0.068	2590.3	155.81
15.5	0.064	2767	146
16	0.06	2857	141
17.5	0.057	3125	129.74

Table 2.12: Peak values for $Maxon\,Bldc\,Ecmax30$ with different possible values of τ

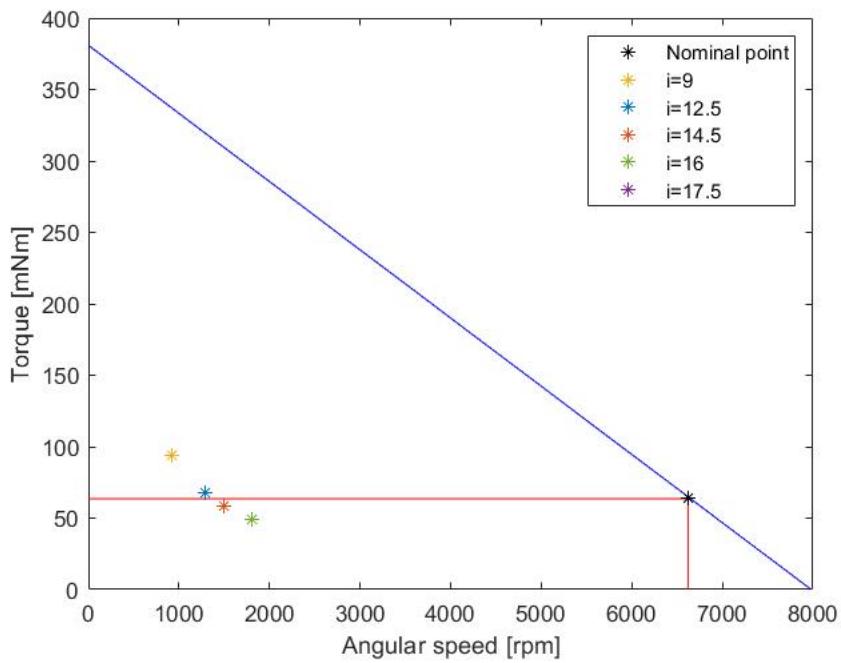

Figure 2.13: Normal operation: Maxon BLDC ECMAX30 mechanical feature in and rms points for different values of τ

Looking to the mechanical feature of the motor, it is clear that there is less useless torque with respect to the previous motor, and the performance are closer to the load conditions.
To avoid to completely change the configuration of the reduction gear, it was decided to mantain the use of normal gears and leadscrew mechanism, working on the gear size to match the selected solution compatible with the available space.
Considering both the worst load conditions, on the basis of the obtained results, it is possible to select a value for the reduction gear ratio in order to proceed for the next step of the design, that is relatd to the reduction gear design and verification.
So:

$$i_{tot} = \frac{1}{\tau} = 16 \tag{2.54}$$

Maintaining the 2-stages reduction gear:

$$i_{1,2} = i_{3,4} = 4 \tag{2.55}$$

Using this gear ratio, in equation 2.56, taken from [12], we define the minimum teeth number for the application:

$$z_{pinion} = \frac{2}{(1+2i)\sin^2(\phi)}\left(i + \sqrt{i^2 + (1+2i)\sin^2(\phi)}\right) = 15.44 \tag{2.56}$$

where ϕ, that is defined as the pressure angle of the tooth, is taken equal to $20°$ (generally selected between $20° - 25°$).
As it is possible to see from tables 2.11 and 2.12, with this value of gear ratio, the $C_{m,rms}$ is lower than motor nominal torque and the $C_{m,max}$ is lower than the motor stall torque.

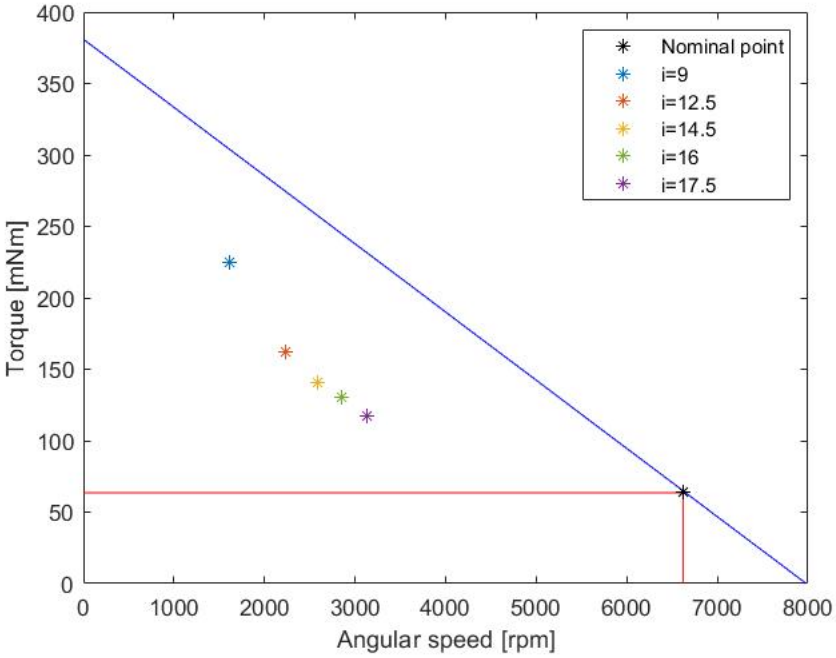

Figure 2.14: Normal operation: Maxon BLDC ECMAX30 mechanical feature and peak points for different values of τ

2.2.4 Reduction gear sizing and verification

For this reduction gear, there are some important parts that need to be verified and controlled: gears, leadscrew and nut, in terms of bending torque and wear, and bearings.

Gear sizing and verification

The selected gears for the application are spur gears with straight teeth and, on the basis of the previous results, the selected number of teeth for each gear are the following:

$$Z_1 = 15 \quad Z_2 = 60 \quad Z_3 = 15 \quad Z_4 = 60 \tag{2.57}$$

with module $m = 0.8$, in order to respect the space constraint.
With this values, the center distance between the pairs of gears is $30mm$: the total horizontal space occupied by the gears, is equal to $90mm$; considering $124mm$ available, we can manage $34mm$ for additional elements.
The last part of the reduction gear, leadscrew and nut mechanism, have been chosen same as the original reduction system.

Starting from the gears, it is fundamental to determine the force acting on each gear in relation to the worst load condition that we have.
The sizing and verification of the gears, have been done considering as worst condition the stall torque of the motor: is a conservative approach, because normally that torque is never reached in normal conditions, but if for some reason the working torque would have reach that value, than the gears would be sized to withstand also such a great force without incurring mechanical features.
In figure 2.15, is represented a graphical scheme for the exchanged force between a pair of gears: speaking about spur gears with straight teeth, all the axial forces components F_x are null.
The stall torque of the motor, as reported previously, is:

$$C_{stall} = 381 \quad [mNm] \tag{2.58}$$

and this torque is directly applied to the first pinion.
Using this torque, considering the pitch diameter of the gear, we can compute the tangential force:

$$\begin{aligned} C_{stall} &= F_t \cdot r_{pitch} \\ F_t &= \frac{C_{stall}}{r_{pitch}} \end{aligned} \tag{2.59}$$

To compute the torque acting on each gear, we need to compute the efficiency of the geared systems as already done in 2.1:

$$\eta_{1,2} = 1 - \frac{1}{2}\left(\frac{1}{Z_1} + \frac{1}{Z_2}\right) = 0.96 \tag{2.60}$$

$$\eta_{3,4} = 1 - \frac{1}{2}\left(\frac{1}{Z_3} + \frac{1}{Z_4}\right) = 0.96 \tag{2.61}$$

So now considering the efficiency, we can compute the torque on each gear using the equation:

$$\begin{aligned} \eta_{n,m} &= \frac{C_m \omega_m}{C_n \omega_n} \\ C_m &= C_1 \cdot \eta_{n,m} \cdot i \end{aligned} \tag{2.62}$$

In table 2.13, the exchanged forces and torques are summarized for each gear.
Starting from those results, we have the target to verify the gears and also to select the material.
The sizing and verification of toothed gears is mainly focused on two mechanical stresses:

- bending fatigue due to the meshing condition
- surface wear due to contact between surfaces

For the detailed calculation of the stresses, it is necessary to refer to current norms and regulations: for this purpose, KHK gears production guide [13] has been useful with the fundamental formulas and norms to compute the important parameters.
The following formulas and computations are based on the JGMA(Japan gear manufacturers association's standards).
Starting with the bending strength, the tangential force applied to the pitch circle F_t must be smaller than the allowable force $F_{t,lim}$:

$$F_t \leq F_{t,lim} \tag{2.63}$$

In addition, also the bending stress at the root, σ_F, must be less than the allowable one $\sigma_{F,lim}$:

$$\sigma_F \leq \sigma_{F,lim} \tag{2.64}$$

For allowable force calculation, the standard norm present the following equation:

$$F_{t,lim} = \sigma_{F,lim} \frac{m_n b}{Y_F Y_\varepsilon Y_\beta} \left(\frac{K_L K_{FX}}{K_v K_o} \right) \frac{1}{S_F} \quad [Kgf] \tag{2.65}$$

instead for the stress equation:

$$\sigma_F = F_t \frac{Y_F Y_\varepsilon Y_\beta}{m_n b} \left(\frac{K_v K_o}{K_L K_{FX}} \right) S_F \quad \left[\frac{Kgf}{mm^2} \right] \tag{2.66}$$

Definition of factors:

- b:facewidth
- Y_F: tooth profile factors
- Y_ε: load sharing factors
- Y_β: helix angle factor
- K_L: life factor
- K_{FX}: size factor of root stress
- K_v: dynamic load factor
- K_o: overload factor
- S_F: safety factor for bending failure

	Gear 1	Gear 2	Gear 3	Gear 4
Torque [mNm]	381	1460.5	1460.5	5598.58
F_t [N]	63.5	60.85	243.41	233.27
F_r [N]	23.1	22.14	88.6	84.9

Table 2.13: Torques and forces acting on the gears

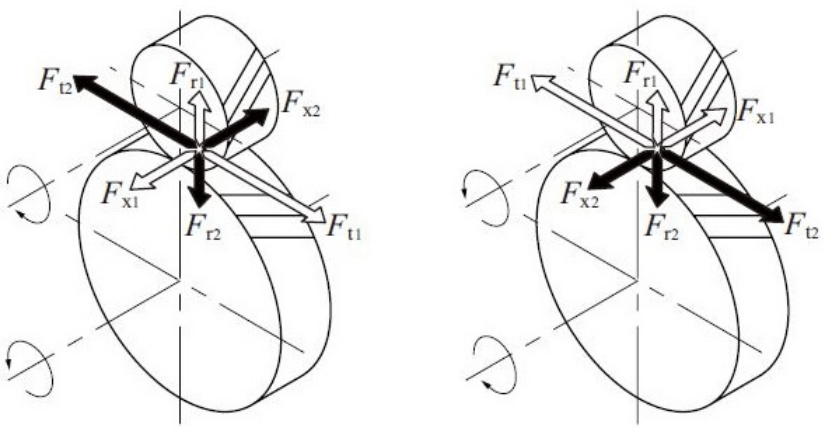

Figure 2.15: Forces exchanged between toothed gears

For what concern the surface wear, the standard is based on the Hertz theory: to guarantee the surface durability, the transmitted tangential force F_t has not to exceed the allowable one $F_{t,lim}$ that is calculated with the allowable Hertz stress. In addition, the actual Hertz stress, σ_H, shall be smaller than the allowable one $\sigma_{H,lim}$.
The allowable tangential force is expressed as:

$$F_{t,lim} = \sigma_{H,lim}^2 d_{01} b_H \frac{i}{i \pm 1} \left(\frac{K_{HL} Z_L Z_R Z_V Z_W K_{HX}}{Z_H Z_M Z_\varepsilon Z_\beta}^2 \frac{1}{K_{H\beta} K_V K_O} \frac{1}{S_H^2} \right) \tag{2.67}$$

instead for the Hertz stress:

$$\sigma_H = \sqrt{\frac{F_t}{d_{01} b_H} \frac{i \pm 1}{i}} \left(\frac{Z_H Z_M Z_\varepsilon Z_\beta}{K_H L Z_L Z_R Z_V Z_W K_{HX}} \sqrt{K_{H\beta} K_V K_O} \right) S_H \tag{2.68}$$

Also here we have to define those factors:

- b_H: effective facewidth to calculate surface strenght
- d_{01}: pinion pitch diameter

- Z_H: zone factor
- Z_M: material factor
- Z_ε: contact ratio factor
- Z_β: helix angle factor
- $K_H L$: life factor
- Z_L: lubricant factor
- Z_R: surface roughnesss factor
- Z_V: lubricatiokn speed factor
- Z_W: hardness ratio factor
- K_{HX}: size factor
- $K_{H\beta}$: longitudinal load distribution factor
- K_V: dynamic load factor
- K_O: overload factor
- S_H: safety factor for pitting

To facilitate the realization of the calculations, has been useful the online tool of KHK gear calculator, that make possible to obtain the allowable stresses and torques substainable by the selected gears: the selected parameters are number of teeth, module, material and all those parameters related to the formulas previously introduced.
Based on the values considered in figure 2.13, being the pair of gears exactly the same between the first and second stage of reduction, the worst condition in terms of stress and torque is on the gears 3 and 4: if those are sized correctly, as a conseguence also the others are correct.
Starting from metal gears, in the table 2.15 are summarized the result obtained. First of all, in green are underlined what are the torques substainable by each gear, parameter important to put in relation to our working conditions: comparing those torques with our working conditions, the gears are correctly sized. The material selected for the first analysis, is a low carbon steel, the S15C (Japanese steel grading), whose chemical composition and mechanical features are reported in table 2.14.

Type	Designation	Chemical composition(%)								
		C	Si	Mn	P	S	C r	Ni	Others	
Carbon steel JIS G 3311 (4051)	S70C	0.65～0.75	0.15～0.35	0.60～0.90	≦0.030	≦0.035	≦0.20	≦0.20	Cu ≦0.30	
	S60C	0.55～0.65	0.15～0.35	0.60～0.90	≦0.030	≦0.035	≦0.20	≦0.20		
	S55C	0.52～0.58	0.15～0.35	0.60～0.90	≦0.030	≦0.035	≦0.20	≦0.20		S55C ～ S15C Ni+Cr ≦0.35
	S50C	0.47～0.53	0.15～0.35	0.60～0.90	≦0.030	≦0.035	≦0.20	≦0.20		
	S45C	0.42～0.48	0.15～0.35	0.60～0.90	≦0.030	≦0.035	≦0.20	≦0.20		
	S15C	0.13～0.18	0.15～0.35	0.30～0.60	≦0.030	≦0.035	≦0.20	≦0.20		

Mechanical Properties

Quantity	Value	Unit
Young's modulus	200000 - 200000	MPa
Tensile strength	650 - 880	MPa
Elongation	8 - 25	%
Fatigue	275 - 275	MPa
Yield strength	350 - 550	MPa

Physical Properties

Quantity	Value	Unit
Thermal expansion	10 - 10	e-6/K
Thermal conductivity	25 - 25	W/m.K
Specific heat	460 - 460	J/kg.K
Melting temperature	1450 - 1510	°C
Density	7700 - 7700	kg/m^3
Resistivity	0.55 - 0.55	$Ohm.mm^2/m$

Table 2.14: S15C material features

Among all the input parameters, the most influent are mainly 2: the gear width and the load factor. For the application, has been chosen a load factor of 1.25, that means to have a load condition not continuosly smooth but with some possible impacts during the operation. The width has been chosen equal to 12mm, this value really affect the strenght of the gear. The safety factor has been chosen equal to 1.2.
Passing to the surface durability, in the table 2.16 are summarized the result obtained as before. Here the important inputs are mainly the number of repetitions, which were assumed to be around 1 million of times, and the kinetic viscosity of the lubricant. Looking to the results, the selected gears can substain the load: to go more in deep, a future step could be a study on the actual fatigue cycles to which the system is subjected and, with those results, evaluate if it is possible to switch to plastic gears to reduce system noise and cost.

Allowable circumferential force (N)	375.46183	510.21385
Allowable torque (N·m)	2.25277	12.24513
Allowable power (kW)	0.47182	0.64115
Normal module	0.8	
Normal pressure angle	20° 0' 0"	
Helix angle	0° 0' 0"	
	Small gear	Large gear
Number of teeth	15	60
Normal tooth profile shift coefficient	0	0
Sum of Normal tooth profile shift coefficient	0	
Transverse contacting pressure angle	20° 0' 0"	
Center distance modification coefficient	0	
Center distance	30	
Pitch circle diameter	12	48
Contacting pitch circle diameter	12	48
Addendum	0.8	0.8
Dedendum	1	1
Tooth height	1.8	1.8
Tool tip roundness radius coefficient	0.38	
Base circle diameter	11.27631	45.10525
Tip diameter	13.6	49.6
Root diameter	10	46
Tooth width	12	12
Transverse contact ratio	< 1.55171 >	
Overlapping contact ratio	0	
Accuracy	JIS 4	JIS 4
Tooth form modification	Modifications	Modifications
Material	S15C	S15C
Heat treatment	Carburizing	Carburizing
Center hardness	HB 150	HB 150
Surface hardness	HV 600	HV 600
Rotational speed(rpm)	2000	500
Peripheral speed (m/s)	1.25654	
Number of repetitions	More or less 1,000,000	
Direction of load	Both directions	
Effective face width	12	12
Tooth form factor	3.10687	2.28632
Load distribution factor along gear tooth	0.64445	
Helix angle factor	1	
Life factor	1.1	1.1
Size factor	1	
Dynamic load factor	1.2	1.2
Overload coefficient	1.25	
Safety ratio	1.2	
Allowable tooth root bending stress(MPa)	128.14023	128.14023

Table 2.15: Bending strenght computations

Allowable circumferential force (N)	283.67666	283.67666
Allowable torque (N·m)	1.70206	6.80824
Allowable power (kW)	0.26736	0.26736
Normal module	0.8	
Normal pressure angle	20° 0' 0"	
Helix angle	0° 0' 0"	
	Small gear	Large gear
Number of teeth	15	60
Normal tooth profile shift coefficient	0	0
Sum of Normal tooth profile shift coefficient	0	
Transverse contacting pressure angle	20° 0' 0"	
Center distance modification coefficient	0	
Center distance	30	
Pitch circle diameter	12	48
Contacting pitch circle diameter	12	48
Addendum	0.8	0.8
Dedendum	1	1
Tooth height	1.8	1.8
Base circle diameter	11.27631	45.10525
Tip diameter	13.6	49.6
Root diameter	10	46
Tooth width	12	82
Transverse contact ratio	< 1.55171 >	
Overlapping contact ratio	0	
Accuracy	JIS 4	JIS 4
Tooth form modification	Modifications	Modifications
Tooth surface finishing methods	Cutting finish	Cutting finish
Tooth surface roughness (Rmax)	12.5	12.5
Material	S15C	S15C
Heat treatment	Carburizing	Carburizing
Center hardness	HB 150	HB 150
Surface hardness	HV 600	HV 600
Rotational speed (rpm)	1500	375
Peripheral speed (m/s)	0.94241	
Kinetic viscosity of lubricant(cSt)	80	
Number of repetitions	More or less 1,000,000	
Direction of load	Both directions	
Method of gear support	Support on both sides(Cannot expect tooth contact)	
Effective face width	12	
Zone factor	2.49457	
Material constant factor (MPa)$^{0.5}$	189.78389	
Contact ratio factor	1	
Helix angle factor	1	
Life factor	1.15	
Lubricant factor	0.98963	0.98963
Roughness factor	0.87986	0.87986
Lubrication speed factor	0.95033	0.95033
Hardness ratio factor	1	1
Size factor	1	
load distribution factor along gear tooth	1.2	
Dynamic load factor	1	1
Overload coefficient	1.25	
Safety ratio	1.2	
Allowable Hertz stress (MPa)	1147.37805	1147.37805

Table 2.16: Surface durability computations

For the last gear, here has been assumed to have a common gear geometry, but from the actuator design the last gear is part of the nut mechanism: in future analysis, will be necessary to study the different geometry to be sure about the sizing and verification.

Leadscrew and nut sizing

In a leadscrew and nut mechanism, an important task, for a correct selection, is the verification of the surface contact pressure in relation to the sliding speed.
The surface contact pressure is calculated as :

$$p = \frac{F}{A_t} \quad [Mpa] \tag{2.69}$$

with F axial force and A_t the total support surface between screw and nut teeth reported on the plane perpendicular to the rotation axis.

The sliding speed is computed as:

$$V_{st} = \frac{V_{tr}}{sen(\alpha)} \quad [m/min] \tag{2.70}$$

that is the ratio between the transaltion speed and the thread inclination angle.
The product between p and V_{st} determine the actual value $p \cdot V$ that is compared with the allowable one, characteristic of the material, the load and operating conditions.
For the allowable values, we need to select the components: the leadscrew and nut, as for the initial actuator configuration, have been selected from Igus catalogue [6] where the technology used for the mechanism is the dryspin, which guarantees a greater conversion of rotating motion into linear motion due to a flatter thread angle with respect to trapezoidal technology; in addition, the wear is reduced due to high material trybological properties, feature of iglidur J that is part of the lubrication free Igus high performance polymers.
In table 2.17, are summarized the useful parameters for the selected nut.
For the surface contact pressure, the axial force has been considered as a mean force on the mechanism, starting from the C_{rms} of the motor previously defined. So, the torque on the last gear, that applies that torque directly on the nut, is computed using the gear ratio and the gears efficiency:

$$C_4 = C_{rms} \cdot \eta_{14} \cdot i_{14} = 53.3 \cdot 0.92 \cdot 16 = 784.5 \quad [mNm] \tag{2.71}$$

The axial force is conseguently:

$$F = \frac{\eta_d \cdot C_4 \cdot 10^{-3}}{R} = \frac{0.64 \cdot 784.5 \cdot 10^{-3}}{0.0019} = 264.9 \quad [N] \tag{2.72}$$

Therefore the actual surface contact pressure is:

$$p = \frac{264.5}{338} = 0.78 \quad [Mpa] \tag{2.73}$$

The translation speed is computed starting from $\omega_{m,rms}$, moving that speed on the last gear and using the transformation ratio R, the speed is easily obtainable:

$$\omega_4 = \frac{\omega_{m,rms}}{i_{14}} = \frac{1649.5}{16} = 103.1 \quad [rpm] \tag{2.74}$$

$$V_{tr} = \omega_4 \cdot R = 103.1 \cdot 0.012 = 1.23 \quad [m/min] \tag{2.75}$$

So the sliding speed:

$$V_{st} = \frac{1.23}{sen(21.54)} = 2.83 \quad [m/min] \tag{2.76}$$

The actual product between p and V_{st} become:

$$p \cdot V_{st} = 2.216 \quad [Mpa \cdot m/min] \tag{2.77}$$

From the material properties in table 2.17, the value of admissible $p \cdot V_{st}$ must be modified in relation to the working conditions: influent factors are the inertia forces, f_i, the working temperature, f_t, and the effective working time with respect to the whole cycle time, f_c.
For the inertia factor, we have to consider that in our application the load and speed can vary a lot during operation and from cycle to cycle: in this conditions, the inertia factor must be chosen between 0.25 and 0.4.
It was difficult to figure out the material characteristic with respect to the environmental temperature, so has been chosen to use a conservative approach: this coefficient should be evaluated from a material graph, but we assumed to use a factor that halves the admissible value.
Finally, the last factor can be evaluated directly from the percentage of motion during the working cycle:

$$f_c = \frac{pause\,time}{working\,time} = \frac{1.3}{0.7} = 1.85 \tag{2.78}$$

Therefore:

$$(p{\cdot}V_{st})_{adm} = (p{\cdot}V_{st})_{max}{\cdot}f_i{\cdot}f_t{\cdot}f_c = 20.4{\cdot}0.33{\cdot}0.5{\cdot}1.85 = 6.22 \quad [Mpa{\cdot}m/min] \tag{2.79}$$

The selected nut is suitable for the application, being the admissible product greater than the actual condition.
The durability verification will have to be deepened to ensure continuous operation.

Igus Nut dryspin JFLM			
inner diameter	10 mm	$\boldsymbol{A_t}$	$338mm^2$
pitch	12 mm	**max p**	35 Mpa
max $\boldsymbol{p \cdot V_{st}}$	20.4 Mpa m/min	**max axial Load**	845 N
thread angle	21.54°		

Table 2.17: Igus drysin nut JFLM

The same durability study shall be performed for the connection between the nut material and the bearings: the system configuration has been designed in order to have that in the last gear reduction stage the screw doesn't receive any radial component, supporting the leadscrew mechanism connecting nut and bearings on both sides, as reported in figure 2.16. In this figure the mechanism is different from the initial model because for the realization of the actual prototype, has been used a different model adapted for the physical implementation of the system.

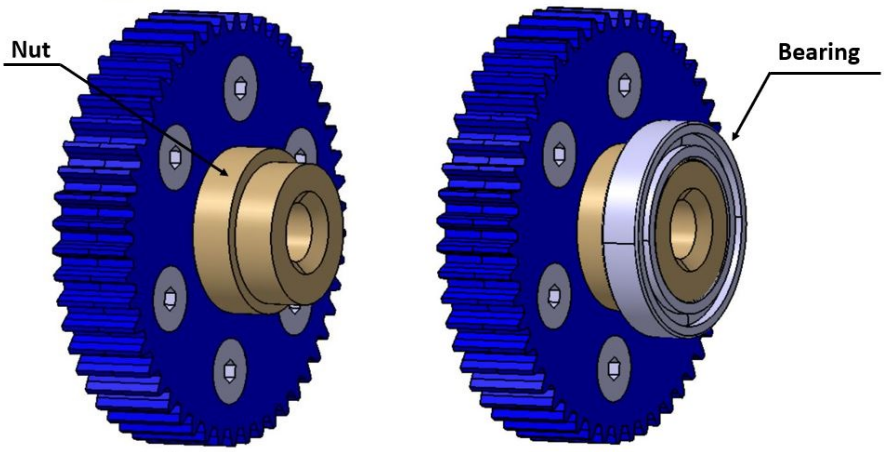

Figure 2.16: Nut and bearings connection

Bearing sizing and verification

In this section, all the calculations are based SKF reference guide and online tools [14]
The load case that has been used for the computations is related to the mean torque and speed given by the motor, so we consider the $C_{m,rms}$ and $\omega_{m,rms}$ previously calculated as input parameters.
Looking to the figure 2.17 (different model as in 2.16), we start from the first two bearings, A and B, on the second shaft, and using the shown reference system it's possible to calculate the exchanged forces between gears.
The values calculated through the known torques and efficiencies are the following:

$$\begin{aligned} F_{t,2} &= \frac{C_2}{r_2} = 8.52 \quad [N] \\ F_{r,2} &= F_{t,2} \tan\alpha = 3.1 \quad [N] \\ F_{t,3} &= \frac{C_3}{r_3} = 34.2 \quad [N] \\ F_{r,3} &= F_{t,3} \tan\alpha = 12.4 \quad [N] \end{aligned} \tag{2.80}$$

where α is the gears pressure angle, that is equal to 20°. Using this forces, it is possible to calculate the reaction forces on the bearings, considering a=12 mm, simply with a couple of equilibrium equation in the x-y and z-x planes.
So:

$$\begin{aligned} R_A &= \sqrt{R_{y,A}^2 + R_{z,A}^2} = 13.3 \quad [N] \\ R_B &= \sqrt{R_{y,B}^2 + R_{z,B}^2} = 21.18 \quad [N] \end{aligned} \tag{2.81}$$

The bearing size can be done with different methods, and here this sizing will be realized based on rating life. The factor that must be determined to make the evaluation are:

- bearing rating life: basic L_{10} and SKF life L_{10m}
- basic dynamic load rating C
- equivalent dynamic bearing load P
- life modification factor a_{SKF}
- lubrication conditions, viscosity ratio k
- fatigue load limit P_u
- contamination factor η_C

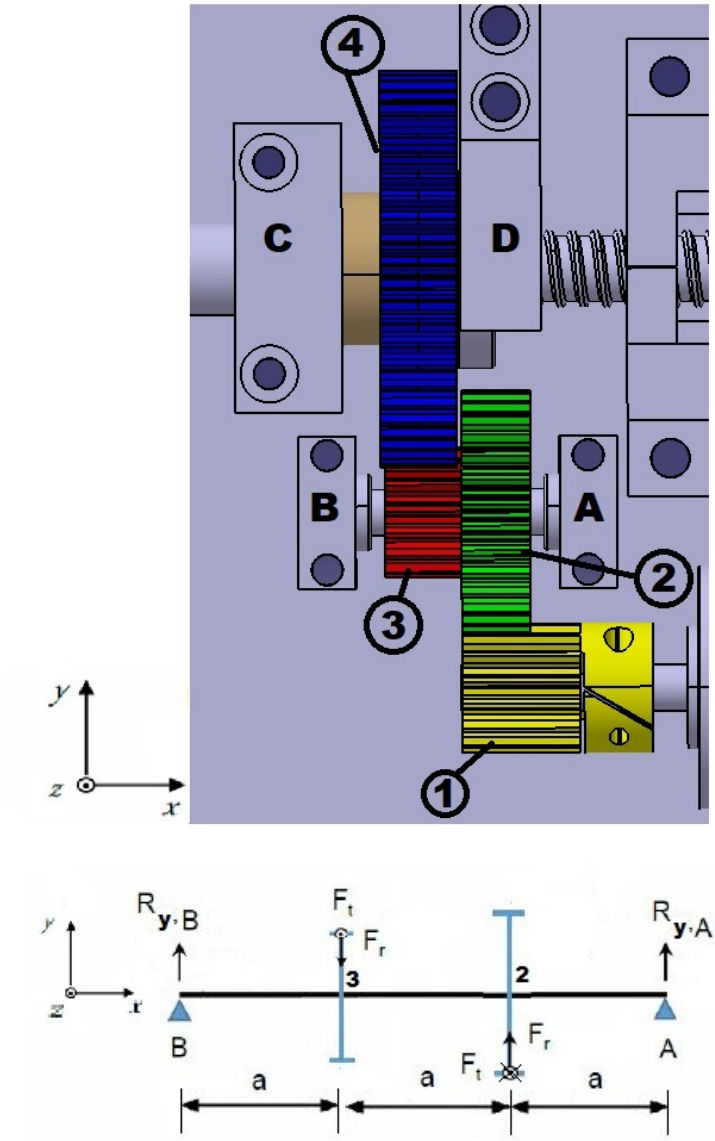

Figure 2.17: Gears and bearing identification and reference system

The basic rating life is defined as:

$$L_{10} = \left(\frac{C}{P}\right)^p \tag{2.82}$$

where p is defined as the exponent of the life equation (generally 3 for ball bearings).

The SKF rating life, instead, considers more factors for the calculation:

$$L_{nm} = a_1 a_{SKF} \left(\frac{C}{P}\right)^p \tag{2.83}$$

where a_1 is defined as life adjustment facotr for reliability (from tables).
So for a reliability of 90%, L_{nm} becomes L_{10m} in millions of revolutions.
The equivalent dynamic bearing load is defined as a hypothetical load, constant in magnitude and direction, that acts radially on a radial bearing and axially and centrically on thrust bearings. If the bearing is loaded simultaneously with radial and axial force, the P is obtained as:

$$P = XF_r + YF_a \tag{2.84}$$

where X and Y are radial and axial load factor for the bearing.
The life modification factor a_{SKF} takes into account different factors for a greater rating life evaluation, like the fatigue load limit in relation to the acting bearing equivalent load, P_u/P, the effect of the contaminations level, η_c, and the lubrication condition. This parameter is evaluated using the diagram 2.20.
For the lubrication condition, must be defined the viscosity ratio k, that is defined as:

$$k = \frac{\nu}{\nu_1} \tag{2.85}$$

where ν is the actual operating viscosity of the lubricant and ν_1 is the rated viscosity, function of the mean bearing diameter and rotational speed. Both can be evaluated from diagrams that take into account the operating temperature and the viscosity grade, that are classified by a norm (ISO 3448). Usually when this ratio is close to one, the advice is that of use additives to reduce the possible wear.
The contamination factor η_c takes into account how the level of solid particle contamination of the lubricant influences the calculated bearing fatigue life. A value close to 1, means parfectly clean conditions, instead closer to 0 menas to have severely contaminated conditions and possible indentations.
To simplify all the calculation, the SKF provide an online tool, the Bearing Calculator,[15].
For the motor shaft, is not necessary to have a bearing also on the opposite side with respect to the motor: for the selected motor, is sufficient the bearing present directly on the stator, with the limitations of a maximum radial force of 25N applied to 5mm from the motor. As seen before, the radial force exerted between gears 1 and 2 is close to 3 N with average torque. Also considering the maximum torque as done for the gear sizing, the force reach 23 N.
So, starting from the second shaft, the two bearings selected for the application are summarized in 2.18, bearings A and B, where are also shown the calculations results. Has been used the same shaft as in the initial actuator configuration, that was sized and verified, with 6 mm of diameter.

Bearing data

	Designation SKF Explorer ▶ Popular item	Bearing type	Principal dimensions Bore d mm	Outer diameter D	Width B	Basic load ratings Dynamic C kN	Static C_0	Fatigue load limit P_u
Left	618/6	Deep groove ball bearing	6	13	3.5	0.715	0.224	0.01
Right	618/6	Deep groove ball bearing	6	13	3.5	0.715	0.224	0.01

Loads & Speed

	Load	Coordinate system	Coordinates x|r mm	y|θ mm|deg	Z mm	Forces Fx|Fr kN	Fy|Fθ kN	Fz kN	Speed r/min	Case weight
LC1	F1	Cartesian	0.0	0.0	12.0	-0.003	0.009	0.0	412.0	1.0
	F2	Cartesian	0.0	0.0	24.0	0.012	-0.034	0.0		

Lubrication

	Designation SKF Explorer ▶ Popular item	Lubricant Type	Method	Name	Effective EP additives	Viscosity @40°C mm²/s	@100°C
Left	618/6	Grease	SKF grease	LGEM 2: high viscosity with solid lubricants	No	500	32
Right	618/6	Grease	SKF grease	LGEM 2: high viscosity with solid lubricants	No	500	32

Bearing rating life

	Designation SKF Explorer ▶ Popular item	Life model Basic L_{10h} h	SKF L_{10mh}	SKF life modification factor a_{skf}	Contamination factor η_c
Left	618/6	> 2x10^5	> 2x10^5	50.0	0.4
Right	618/6	> 2x10^5	> 2x10^5	8.99	0.4

Lubrication conditions

	Designation SKF Explorer ▶ Popular item	Operating viscosity Actual ν mm²/s	Rated ν_1	Rated @ 40 °C ν_{ref}	Viscosity ratio K
Left	618/6	124	85.3	311	1.45
Right	618/6	124	85.3	311	1.45

Figure 2.18: Bearings A and B summary

Starting with the load application, the forces F_x and F_y represent respectively the radial and tangential force. The speed has been considered as mean speed on the second shaft: the mean motor speed is equal to $1649.5rpm$, with a gear ratio equal to 4, the mean speed is $412rpm$.

Passing to the lubrication, from she SKF lubrication specification method, has been selected a grease with high viscosity, which acronym is tabulated as LGEM2,[14]: is a lubricant with high viscosity and solid lubricants that is suitable for conditions with peak loads and frequent startup, similar to our applications.
The bearing rating life is sufficient to guarantee an application that is able to satisfy the requirements of long life service, as the vehicle life, without replacement of parts.
For a_{SKF} we have the two bearings in zone B and C of the relative graph in 2.20: both bearings are lightly loaded.
The contaminations factor, considering our application, has been selected a condition of "slight contamination", that means to have bearings without integral seals, wear particles and slight ingress of contaminants.
Passing to the bearings C and D, we compute the force on the last gear: in this case we have both radial forces and axial forces on the bearings, because we have the radial component that is given by the gear and the axial component given by the leadscrew and nut mechanism.
For the gear, the forces are:

$$\begin{aligned} F_{t,4} &= \frac{C_4}{r_4} = 32.7 \quad [N] \\ F_{r,4} &= F_{t,4} \tan\alpha = 11.9 \quad [N] \end{aligned} \tag{2.86}$$

For the leadscrew and nut, as done for the gear, we consider a mean load:

$$F_{axial} = \frac{C_4 \eta_d 2\pi 1000}{P} = 265 \quad [N] \tag{2.87}$$

As before, we use the SKF online tool for the bearings calculation.
The bearing data are summarized in 2.19. For the calculations, it was necessary to select just one bearing that must support the axial load: considering that the worst load case is when the actuator must actuate 556N (see next section) with verse from bearing C to bearing D, the right bearing D has been selected to substain that axial load.
Here the speed is again reduced by the gear ratio, up to $103rpm$.
The lubrication, is the same as before, except for the use of EP additives: those are additives for "extreme pressure" that the SKF recommends for viscosity ratio lower than 1, condition that can arise when the speed is very low, the lubricant viscosity is not sufficient or the cooling is not appropriate.
The contamination factor has been selected equal to the other bearings couple.

Bearing data

	Designation SKF Explorer ▶ Popular item	Bearing type	Principal dimensions Bore d	Outer diameter D	Width B	Basic load ratings Dynamic C	Static C_0	Fatigue load limit P_u
			mm			kN		
Left	61901	Deep groove ball bearing	12	24	6	2.91	1.46	0.062
Right	61901	Deep groove ball bearing	12	24	6	2.91	1.46	0.062

Loads & Speed

	Load	Coordinate system	Coordinates x|r	y|θ	Z	Forces Fx|Fr	Fy|Fθ	Fz	Speed	Case weight
			mm	mm|deg	mm	kN	kN	kN	r/min	
LC1	F1	Cartesian	0.0	0.0	20.0	0.012	0.033	0.265	103.0	1.0

Lubrication

	Designation SKF Explorer ▶ Popular item	Lubricant Type	Method	Name	Effective EP additives	Viscosity @40°C	@100°C
						mm²/s	
Left	61901	Grease	SKF grease	LGEM 2: high viscosity with solid lubricants	Yes	500	32
Right	61901	Grease	SKF grease	LGEM 2: high viscosity with solid lubricants	Yes	500	32

Bearing rating life

	Designation SKF Explorer ▶ Popular item	Life model Basic L_{10h}	SKF L_{10mh}	SKF life modification factor a_{skf}	Contamination factor η_c
		h			
Left	61901	> 2x10^5	> 2x10^5	50.0	0.4
Right	61901	98800	183000	1.86	0.4

Lubrication conditions

	Designation SKF Explorer ▶ Popular item	Operating viscosity Actual ν	Rated ν_1	Rated @ 40 °C ν_{ref}	Viscosity ratio K
		mm²/s			
Left	61901	270	204	365	1.32
Right	61901	270	204	365	1.32

Figure 2.19: Bearings C and D summary

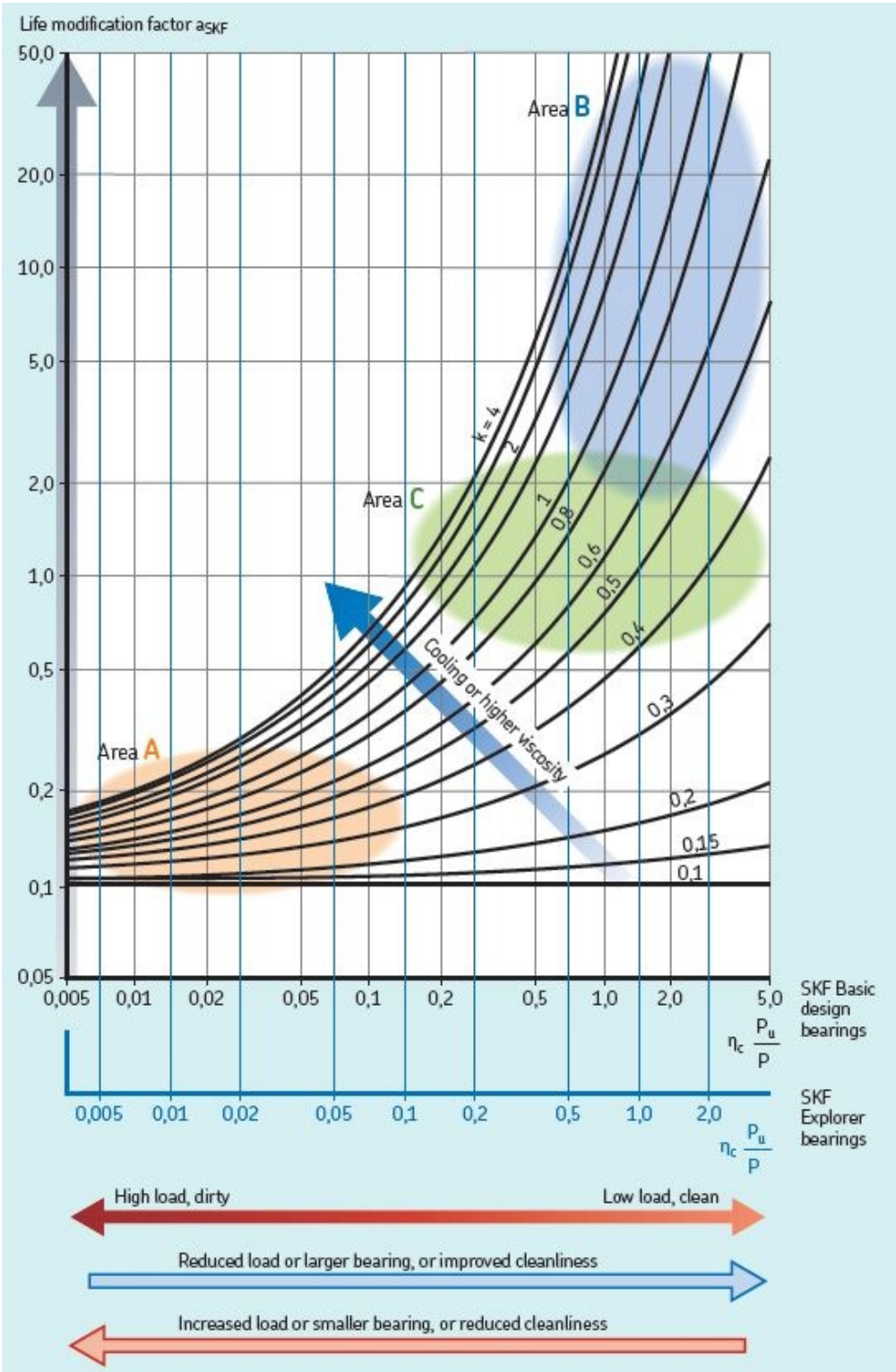

Figure 2.20: a_{SKF} life modification factor

2.3 P Emergency safety function unit

The actuator shall be equipped with an emergency unit, called P emergency safety function unit, in order to guarantee a mechanical activation of the parking lock in case of a fault. At the same time, the system shall be restored without any kind of external human action, but simply, when the fault is repaired, through the use of the dc motor, a sort of electromechanical restoring.
In the image 2.21, we have a focus on the system: the bigger spring is the mechanical energy storage device that must actuate the needed force, then the two levers that mantained the spring compressed(in green) are connected between each other through two bracket with teethed profile, so they can rotate when necessary; in brown we have the shaft that mantains the levers blocked and finally, in yellow, we have the electromagnet, that retains the whole system in charge.
In figure 2.22, it is more clear the connection between the green levers.
So from images 2.21 and 2.22 it is possible to understand that, when there is not current, the electromagnet releases the brown shaft, that enable the rotation of the two green levers and, conseguently, the spring expands itself moving the light blue part, that is mechanically connected to the screw
So, first of all we need to design properly the spring in order to guarantee the necessary load at the output, 200N, considering all the losses that we have in the middle, mainly related to the leadscrew mechanism, reduction gears and friction forces.
Starting from a static sizing, we need to define our input parameters: of course we need to design the spring considering force to actuate, available compression and lenght, available internal and external diameters. In the image 2.23, are summarized the characteristic dimensions of a generic compression spring: for geometrical constraint, we have that the inner diameter could not be smaller than 16.5 mm (D_i) and the lenght L_2, where we will exploit the actuation force, could not be greater than 41 mm. So, we start from the definition of the material, that for springs is generally a carbon steel: the one used for the calculation is the C98, for which the characteristic are summarized in table 2.19. The spring stiffness, can be calculated like:

$$k = \frac{Gd^4}{8D^3n} \quad \left[N/mm\right] \tag{2.88}$$

where G is the shear modulus of the material, d is the wire diameter, D is the average diameter and n is the number of active coils.
These parameters can be chosen quite freely, with the exception of the average diameter where there is the limit of 16.5 mm for what concern the inner diameter.

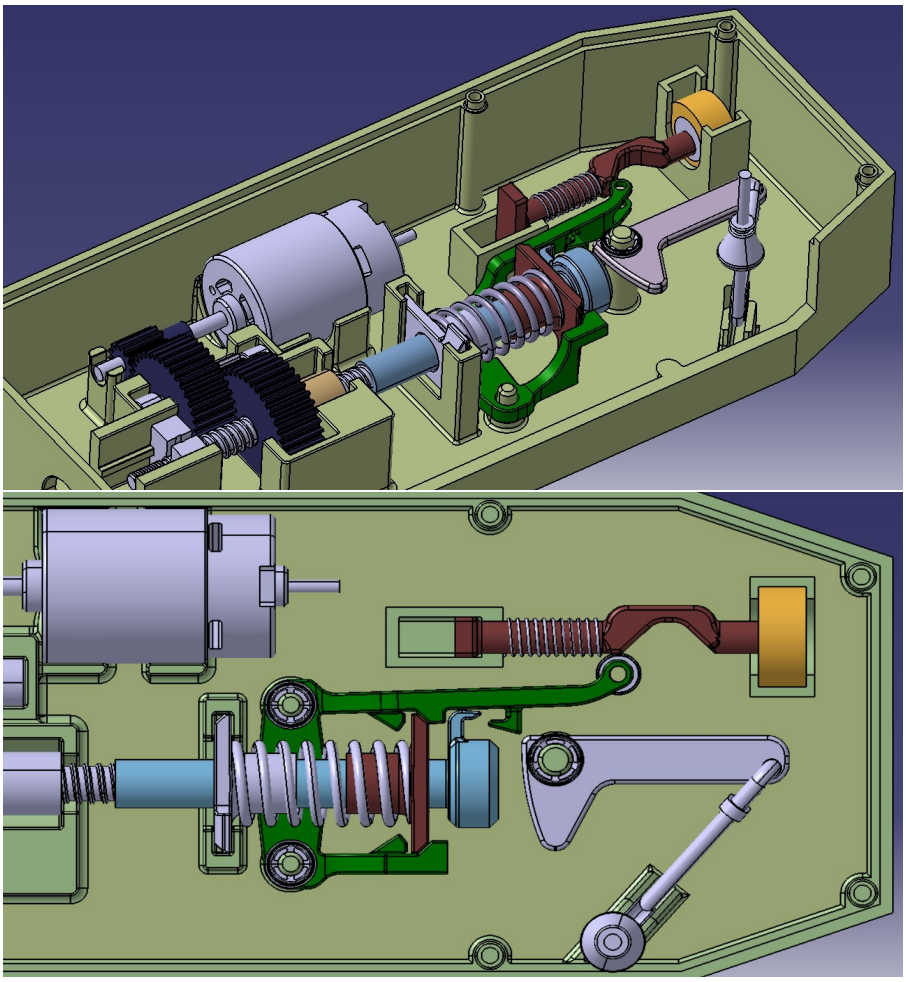

Figure 2.21: P emergency safety function unit

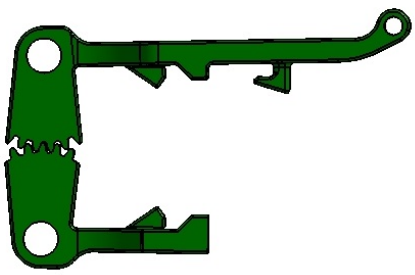

Figure 2.22: Mechanical rotational levers of the emergency unit

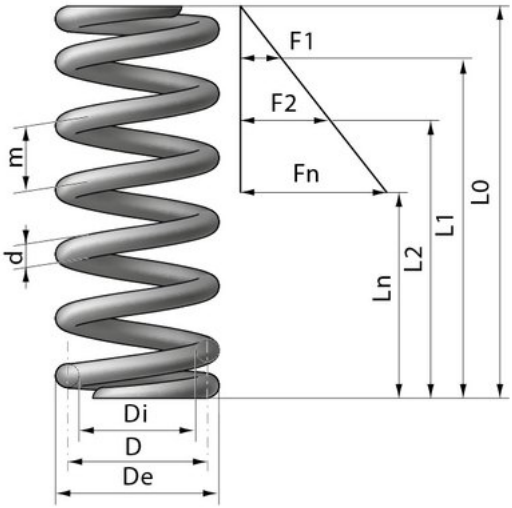

Figure 2.23: Compression spring characteristic dimensions

The spring lenght in compression state is equal to 32 mm. The force exploited by the spring will be:

$$F_2 = k(L_0 - L_2) \tag{2.89}$$

with reference to 2.23.
Instead the preload force is:

$$F_1 = k(L_0 - L_1) \tag{2.90}$$

where L_1 will be the spring in compression L_2 plus the travel of the actuator, 12.5mm. So the free lenght is another key parameter in the choice. In the leadscrew mechanism, we have a lot of losses due to the low efficiency of the mechanism it self, so we have to calculate what is the torque that is needed by each part of the transmission that is directly attached to the screw through the nut: in this way, we compute which is the starting torque or, better, the static friction torque that has to be win to put the system in rotation.
This will define an extra force in addition with respect to the 200N needed by the load.
Using the data obtained through the bearings calculations, directly on them we have which is the static friction torques, that of course are a conseguence of the radial and axial load applied to the gears.
In the bearings C and D, where we have the nut, the friction torque is reported in figure 2.24.

Bearing friction & power loss

	Designation	Frictional moment		Friction sources				Power loss
	SKF Explorer	Total	At start 20-30°C and zero speed	Rolling	Sliding	Seals	Drag loss	
	▶ Popular item	M	M_{start}	M_{rr}	M_{sl}	M_{seal}	M_{drag}	P_{loss}
		Nmm						*W*
Left	61901	0.22	0.02	0.21	0.01	0	0	0
Right	61901	7.38	7.91	3.05	4.32	0	0	0

Figure 2.24: Friction torque for bearings C and D

So considering the total value of the friction torque, M total, we consider both the starting torque and the dynamic torque needed during the travel. For the second couple of bearings, A and B, the same values are shown in figure 2.25.

Bearing friction & power loss

	Designation	Frictional moment		Friction sources				Power loss
	SKF Explorer	Total	At start 20-30°C and zero speed	Rolling	Sliding	Seals	Drag loss	
	▶ Popular item	M	M_{start}	M_{rr}	M_{sl}	M_{seal}	M_{drag}	P_{loss}
		Nmm						*W*
Left	618/6	0.06	0.0	0.06	0.0	0	0	0
Right	618/6	0.17	0.08	0.12	0.04	0	0	0

Figure 2.25: Friction torque for bearings A and B

Also the motor, being switched off, has its own rotor friction torque: unfortunately is not a data available on the motor data sheet, so for now we will consider a certain safety coefficient on the total torque needed by the transmission to include also that contribution.

The total torque needed in the output shaft, related to the bearings C and D, without any external load, is equal to 7.41 Nmm.
For the torque in second shaft, related to bearings A and B, we have to move that torque to the output shaft considering the transmission ratio and gear efficiency:

$$M_{AB} = 0.23 \quad [Nmm] \tag{2.91}$$

moved to the screw shaft:

$$M'_{AB} = \frac{M_{AB} * i}{\eta} = \frac{0.51 \cdot 4}{0.98} = 0.938 \quad [Nmm] \tag{2.92}$$

The total torque moved to the output shaft is:

$$M_{tot} = M'_{AB} + M_{CD} = 8.53 \quad [Nmm] \tag{2.93}$$

Now, considering the leadscrew and nut mechanism, we can compute the axial force to be applied to the screw to put in rotation the gears. Starting from the retrograde efficiency of the mechanism, defined as translational input from the screw, rotational output of the nut:

$$\eta_r = \frac{M_{tot} \cdot \omega}{F_{spring} \cdot V} \tag{2.94}$$

so

$$F_{spring} = \frac{M_{tot}}{R \cdot \eta_r} = \frac{8.53 \cdot 10^-3}{0.0019 \cdot 0.52} = 8.63 \quad [N] \tag{2.95}$$

where R has been defined in the previous section as the transformation ratio of the leadscrew and nut mechanims. In the calculation should be considered also the inertia of the gears, but considering that the friction contribution is the most influent in such small gears. Using a safety coefficient of 3-5 to take into account all the possible extra contributions present in the actual case, this force is increased:

$$F_{spring} = 13.44 \cdot 3 = 40.32 \quad [N] \tag{2.96}$$

Starting with this value, we can design properly the spring. The calculations are summarized in table 2.18, where are highlighted the force values in maximum and preload compression: the max force has been further increased, because for the unlocking it is needed an additional force to win friction forces.

INPUT				OUTPUT			
Geometric data				*Block lenght*	Lb	mm	21
Wire diameter	d	mm	3	*Coils pitch*	p	mm	6.4
Internal diameter	Di	mm	16.8	*Medium diameter*	Dm	mm	19.8
External diameter	De	mm	22.8	*Wrapping ratio*	c	#	6.6
Free lenght	L0	mm	47.7	*Spring stiffness*	k	N/mm	17.7
Preload lenght	L1	mm	44.5	*Preload Force*	Fpre	N	56.7
Compressed spring lenght	L2	mm	32	*Max Force*	Fmax	N	278.2
Min operating lenght	Lmin	mm	3.2	*Min Force*	Fmin	N	56.7
Max operating lenght	Lmax	mm	15.7	*Wahl Factor*	kb	#	1.227
Active coils	i	#	6	*Max stress*	Smax	Mpa	637.4
Total coils	Ti	#	7.5	*Min stress*	Smin	Mpa	129.9
Material data				*Mean stress*	Smean	Mpa	383.7
Material name			C98				
Tan Modulus	G	Mpa	81500				

Table 2.18: Main spring calculation data

Now, to verify the spring design, the general procedure, reported in [12], has 2 key passages: static resistance and fatigue resistance.

For the static resistance,we have that:

$$\tau_{max} = \lambda \frac{8F_{max}D}{\pi d^3} \leq \tau_{adm} \tag{2.97}$$

where λ it's called Wahl factor, and is computer as:

$$\lambda = \frac{4c-1}{4c-4} + \frac{0.615}{c} \tag{2.98}$$

with c called characteristic ratio D/d, that should be between $7 \div 12$ in order to be optimal.

C	Si	Mn	P	S	Cu
0.45-1.00	0.10-0.30	0.50-1.20	0.020 max	0.025 max	0.12 max

Density	Elastic Modulus E	Shear modulus G	Working temperature
7.85 Kg/dm3	206 KN/mm2	81.5 KN/mm2	-30 +100 °C

Table 2.19: C98 spring steel chemical composition and mechanicl properties

Defining R_m as the tensile strenght, which depend also on the wire diameter, the τ_{adm}, called the admissible stress, is calculated, for cold drawn materials, as:

$$\tau_{adm} = 0.5R_m \tag{2.99}$$

The R_m depends not only on the material type, but also on the wire diameter: using a 3mm wire, the relative value of R_m is equal to 1950 Mpa. So:

$$\tau_{adm} = 975 \quad [Mpa] \tag{2.100}$$

and looking to the maximum stress present in 2.18:

$$\tau_{max} = 637.4 \leq 975 = \tau_{adm} \quad [Mpa] \tag{2.101}$$

For the fatigue resistance instead, the verification to do is the following:

$$\Delta\tau_{nom} = \lambda \Delta F \frac{8D}{\pi d^3} \leq \Delta\tau_{adm} \tag{2.102}$$

where ΔF is the difference between F_{max} and F_{min}, while $\Delta\tau_{adm}$:

$$\Delta\tau_{adm} = b_d \Delta\tau_0 - b_\tau \tau_{min} = 387.21 \quad [Mpa] \tag{2.103}$$

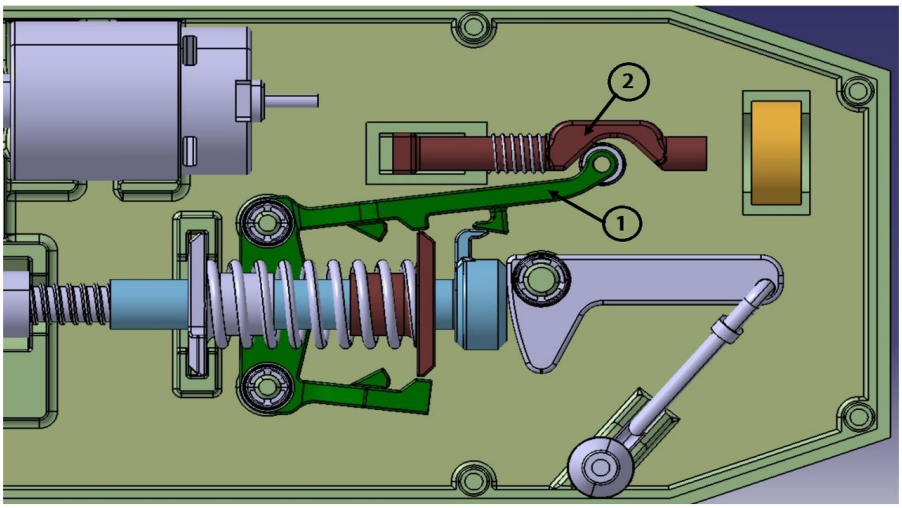

Figure 2.26: P emergency safety function unit in released state

The coefficients b_τ and $\Delta\tau_0$ are tabulated values that depend upon the material selection and his surface treatment, b_d instead depends in the wire diameter.
For the calculations, have been used:

$$b_d = 1 \quad b_\tau = 0.18 \quad \Delta\tau_0 = 410 \quad [Mpa] \tag{2.104}$$

Instead, as regards τ_{min}, it's calculated as:

$$\tau_{min} = \lambda''' \frac{8F_{min}D}{\pi d^3} \tag{2.105}$$

where λ''' is called corrective factor for shear effects, computed as:

$$\lambda''' = 1 + \frac{0.5}{c} \tag{2.106}$$

Again, considering the values in table 2.18, the fatigue is verified:

$$\Delta\tau_{nom} = 383.7 \leq 387.21 = \Delta\tau_{adm} \quad [Mpa] \tag{2.107}$$

After the spring sizing, now we have to make some consideratiosn on the emergency mechanism: going back to the image 2.21, the system as is now designed, does not guarantee the restoring of the system in stable position.
It is more clear to look the figure 2.26.

Looking to it, we can see that without a mechanical connection between the green levers, component 1, and the brown shaft, component number 2, is not possible to restore the system and the electromagnet, component in yellow, when the current return available again.

When the power supply is again available, the motor will start to move and conseguently, moving all the system to the left, we need to modify the mechanism to obtaine an automatically restoring system.
To doing so, the green levers have been modified as shown in figure 2.27: by means of the connection between the levers, obtained by means of sectors of spur gears, increasing the sector dimension, it is possible to take an advantage of the levers rotation to have a connection with the electromagnet shaft. This connection is made possible by adding two additional spur gears, in yellow, an idle gear (Z=17) to reverse the motion and one to connect the motion to the rack added to the electromagnet shaft (Z=40). The rack is fitted on a small linear guide to provide the possible of horizontal motion. The missing parts are just hidden to show the modified configuration.
The force that the spring exerts on the green levers, is exchanged through inclined planes at 45°: taking again the image in the equivalent wedges in figure 2.6, but adding the friction on the constraints.
Supposing to have an equal coefficient of friction in all the constraints, the formula that can be used is the following:

$$\frac{F_{spring}}{F_{45}} = \tan(\alpha + 2\phi) \tag{2.108}$$

and with a coefficient of friction of 0.15 (lubricated steel), the relative ϕ is equal to:

$$\phi = \tan^{-1}(f) = 8.53° \tag{2.109}$$

so the force at 45°:

$$F_{45} = \frac{278.2}{\tan(45 + 2 \cdot 8.53)} = 147.5 \quad [N] \tag{2.110}$$

In figure 2.28, in the first picture, are reported schematically the exchanged forces, where the F_{45} creates a torque in the green levers, and considering that the arm of the torque around the rotation point of the levers is 20mm:

$$T = F_{45} \cdot r = 2.95 \quad [Nm] \tag{2.111}$$

That torque, passes through the two gears and, considering an efficiency of 0.98 for both gears:

$$\begin{aligned} T_1 &= \eta_{01} \cdot T \cdot i_{01} = \eta_{01} \cdot \cdot T \frac{17}{40} = 0.98 \cdot 2.95 \cdot 0.425 = 1.23 \quad [Nm] \\ T_2 &= \eta_{12} \cdot T_1 \cdot i_{12} = \eta_{12} \cdot T_1 \cdot \frac{40}{17} = 0.98 \cdot 1.23 \cdot 2.35 = 2.83 \quad [Nm] \end{aligned} \tag{2.112}$$

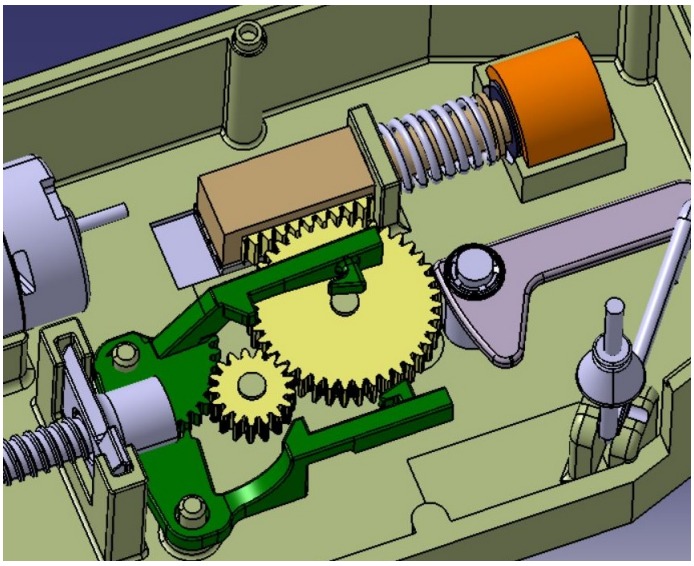

Figure 2.27: Modified P emergency safety function unit

The last gear, with a pitch diameter of 40mm, exerts a force on the rack equal to:

$$F_{t,rack} = \frac{T_2}{r_{pitch}} = 141.81 \quad [N] \tag{2.113}$$

To mantain the system blocked, the reaction force given by the electromagnet attraction and by the contrast spring, must be greater than $F_{t,rack}$.
For the purpose, has been decided to use a combination that guarantees at least $F_{react} = 160N$, using an electromagnet able to apply 60N when powered, and a spring with 100N of preload.
The selected electromagnet is reported in 2.29 [16]: the manufacturer guarantees that the electromagnet is able to sustain a maximum ambient temperature of $80°C$, above this value could be damaged or can lose magnetism.
The second spring data are summarized in 2.30.

When the power supply is not available anymore due to a fault, on the reaction side we lose the contribution of the attraction force of the electromagnet, so the force exerted by the main spring is sufficient to release the emergency system.
When the power returns again available and the dc motor moves the screw on the left, the reaction spring force is sufficiently high to put again in position the release mechanism, this because the force of the main spring is temporarily overshadowed by the motor force, like reported in the second image in 2.28.

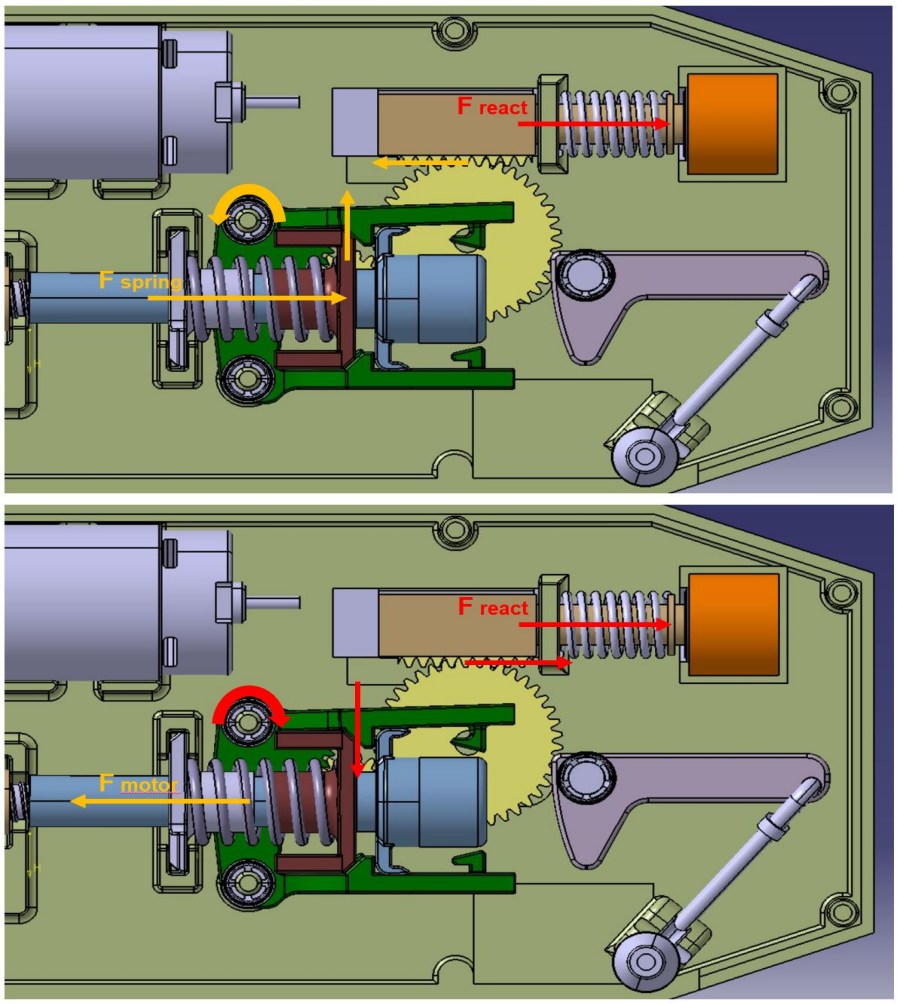

Figure 2.28: Forces exerted in the emergency mechanism

The rack is installed on a block that can move linearly on the actuator plane by means of a rail and guide carriage.
The radial force that is exerted on the rack is:

$$F_{r,rack} = F_{t,rack} \tan(\alpha) = 141.81 \cdot \tan(20) = 51.61 \quad [N] \tag{2.114}$$

That radial force in the rack, creates a friction force between the carriage and the guide: considering that the selected guide and carriage, as in figure are again Igus products, it is available the static coefficient of friction between the material of the carriage, iglidur J, and steel.

Weight: 50 g
Haltekraft: 60 N
Anzugsplattendicke: 2,5 mm

Coil Data

Duty (%)	100	–	–	–
Power Drain (Watt)	4	–	–	–
Max. Duty (Seconds)	∞	–	–	–

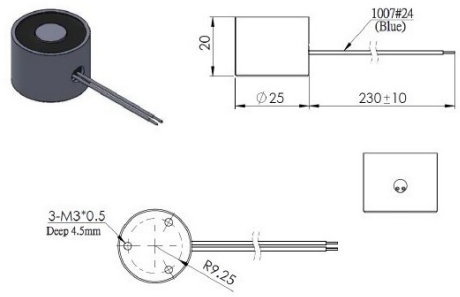

Figure 2.29: Electromagnet data

INPUT				OUTPUT			
Geometric data				*Block lenght*	Lb	mm	14
Wire diameter	d	mm	2	*Coils pitch*	p	mm	4.9
Internal diameter	Di	mm	12.5	*Medium diameter*	Dm	mm	14.5
External diameter	De	mm	16.5	*Wrapping ratio*	c	#	7.25
Free lenght	L0	mm	37	*Spring stiffness*	k	N/mm	8.9
Preload lenght	L1	mm	36	*Preload Force*	Fpre	N	8.9
Compressed spring lenght	L2	mm	25	*Max Force*	Fmax	N	106.9
Min operating lenght	Lmin	mm	1	*Min Force*	Fmin	N	8.9
Max operating lenght	Lmax	mm	12	*Wahl Factor*	kb	#	1.205
Active coils	i	#	6	*Max stress*	Smax	Mpa	594.6
Total coils	Ti	#	7.5	*Min stress*	Smin	Mpa	49.6
Material data				*Mean stress*	Smean	Mpa	322.1
Material name			C98				
Tan Modulus	G	Mpa	81500				

Figure 2.30: Reaction spring calculation data

This value is considered $\mu_s = 0.18 \div 0.25$ with a motion between iglidur J and steel.
The friction force, in static conditions, is equal to:

$$F_{frict} = F_{r,rack} \cdot \mu = 51.61 \cdot 0.25 = 12.75 \quad [N] \tag{2.115}$$

The total reaction force is:

$$F_{react} = F_{rspring} + F_{magnet} + F_{frict} = 106.9 + 60 + 12.7 = 179.6 \quad [N] \tag{2.116}$$

The details about iglidur material and Igus solutions are easily accessible on the website and on [6].

When the system is in normal operation and the parking lock is engaged, when the car is swithced off, to avoid to have the unwanted emergency actuation, are

used two hooks on the light blue shaft that mantain the green levers blocked, like reported in 2.31. To be certain about the design and sizing, the system must be realized and properly tested.

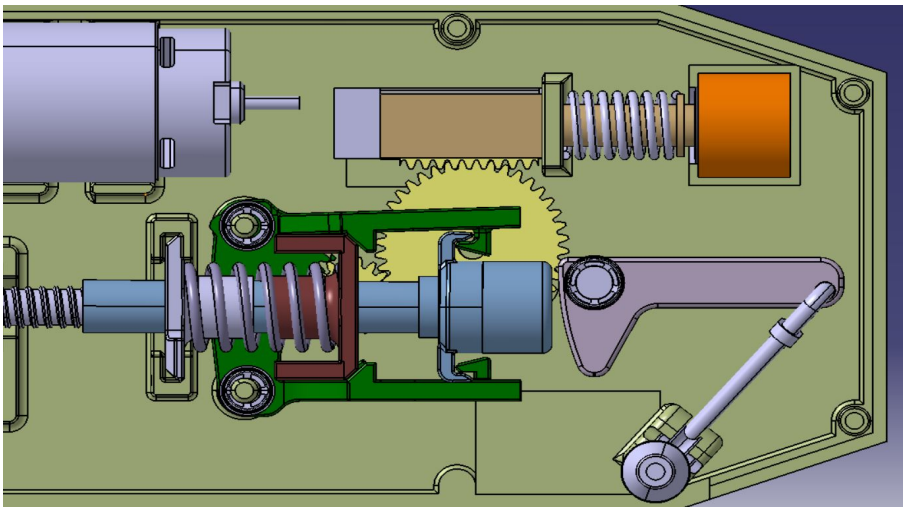

Figure 2.31: Vehicle in parking and emergency system blocked

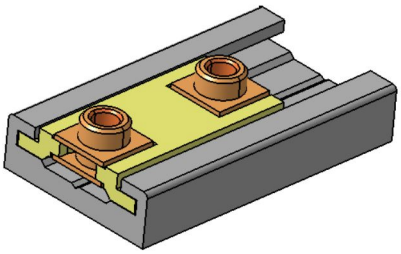

Figure 2.32: Igus guide and carriage

Chapter 3

Basic simulations and tests

In order to have a first possible test of the actuator, a base point for the performance evaluation, has been useful to exploit the simulation softwares available through the academic licenses, Matlab and Simscape. Unfortunately, neither in its starting configuration, was not possible to simulate physically the actuator: the test for which was possible an actual simulation, has been the emergency system, in order to have a verification for what concern the spring sizing, but without any kind of electrical control or power source, like reported in the next section.

3.1 Actuator virtual simulations

Using Simscape driveline and electrical, it is possible to obtain simulations of electromechanical systems: the Simscape environment is an extension of Simulink, with tools for modeling and simulating multidomain physical systems. With respect to the analytical computations, here the load simulation is much more close to the actual situation: in the previous computations has been used a conservative approach for which, in the 2 steps of the motion profile, the torque needed by the load has been considered as constant during the steps, but this is not true in the actual situation, because the load profile decreases in the first millimeters of travel without a perfect linearity.
In figure 3.1 is represented the scheme used for the simulations: on the left, we have the electrical part, that is always represented in blue, then we have the Dc motor in the middle, a mid point between electrical and mechanical fields and than on the right side all the mechanical components. The load simulation is realized using a non linear translational spring, that is able to simulate a different stiffness along the travel, that is exactly what we need to test. To introduce the load schematization is sufficient to build an excel file with plausible values: being the exact load profile not available in the customer specification, the known points are the starting and the ending one.

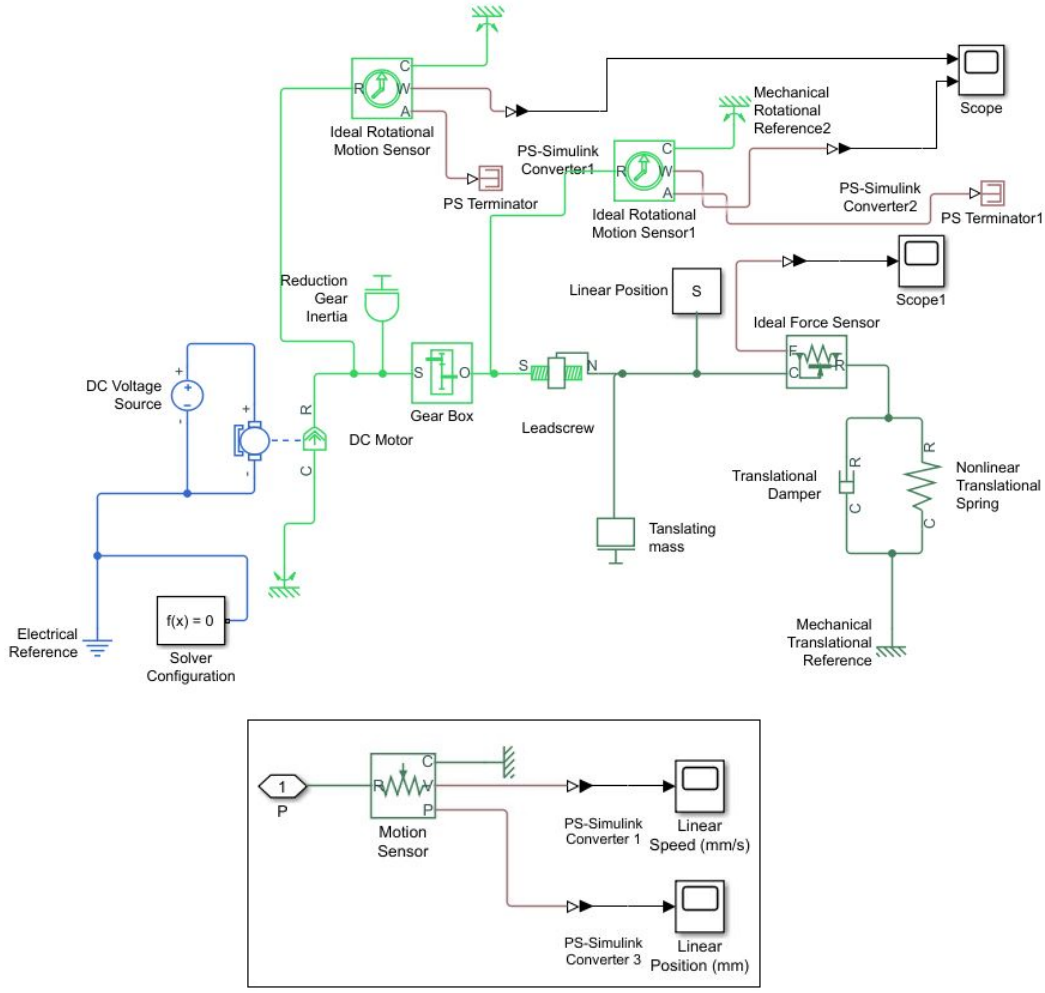

Figure 3.1: From the top: Simscape simulation and S motion sensor schemes

To have a more representative simulation, have been added the value of the translating mass, mainly related to the screw , and the value of the reduction gear inertia, moved to the drive shaft. In the leadscrew, it is possible to introduce the pitch and the efficiencies value, both direct and inderect one.
In order to evaluate the effective motion at the output shaft, a linear position sensor has been introduced: it is a subsystem containing, second image in figure 3.1, the actual motion sensor and the PS-simulink converter to convert quantities from Simscape environment to Simulink environment, in order to show the desired quantities through the scopes.
In the electrical part, we have just the dc voltage source and the electrical reference. The first load case simulated is the worst load condition in normal operation, for

which has been supposed a profile, like depicted in figure 3.2, and the excel values used for that graph have been used in the non linear spring.
The results are shown in figure 3.3: starting from the motor results, it is possible from the simulation to see the current absorption, torque, power supply voltage and speed.
In this phase the 2 important parameters are mainly torque and current absorption: the starting current, is the peak current that for this motor is within the target of 30 A, and the torque is close to that one calculated analytically.
Through the motion sensor, it is possible to monitor the motion of the output of the actuator, in order to evaluate if we reach the needed travel in relation to the load: it is possible to notice, always in figure 3.3, that in less than 0.15 seconds we reach the desired travel, but, of course, we have to consider that here we do not have implemented all the control strategy for the motor brake phase and, in addition, here we do not evaluate the motor and load coupling in terms of *rms* torque and speed but just for what concerns peak values.
The simulation is not representative in terms of actual function, but it is really important in order to evaluate the mentioned parameter in temporal trend.
Passing to the other load case, in emergency condition, the simulated load is represented in figure 3.4: as explained in the previous chapter, the difference here is mainly related to the force that we have to guarantee along all the travel, till the end of spring compression. The load starts from an higher value, with respect to the normal operation, due to the spring preload in released state, decrease for some millimeters, and then rise again reaching the value of the spring force in compressed state. As before, we can evaluate the motor current absorption, delivered torque and linear motion as shown in figure 3.5.

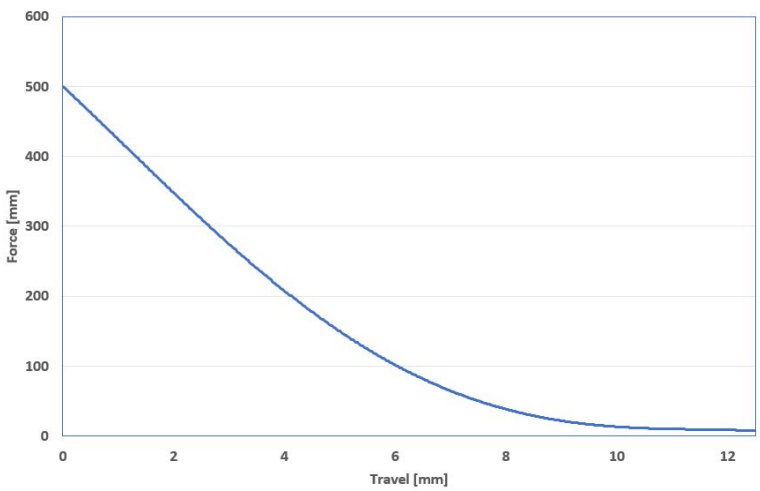

Figure 3.2: Supposed worst case load profile in normal operation for non linear spring

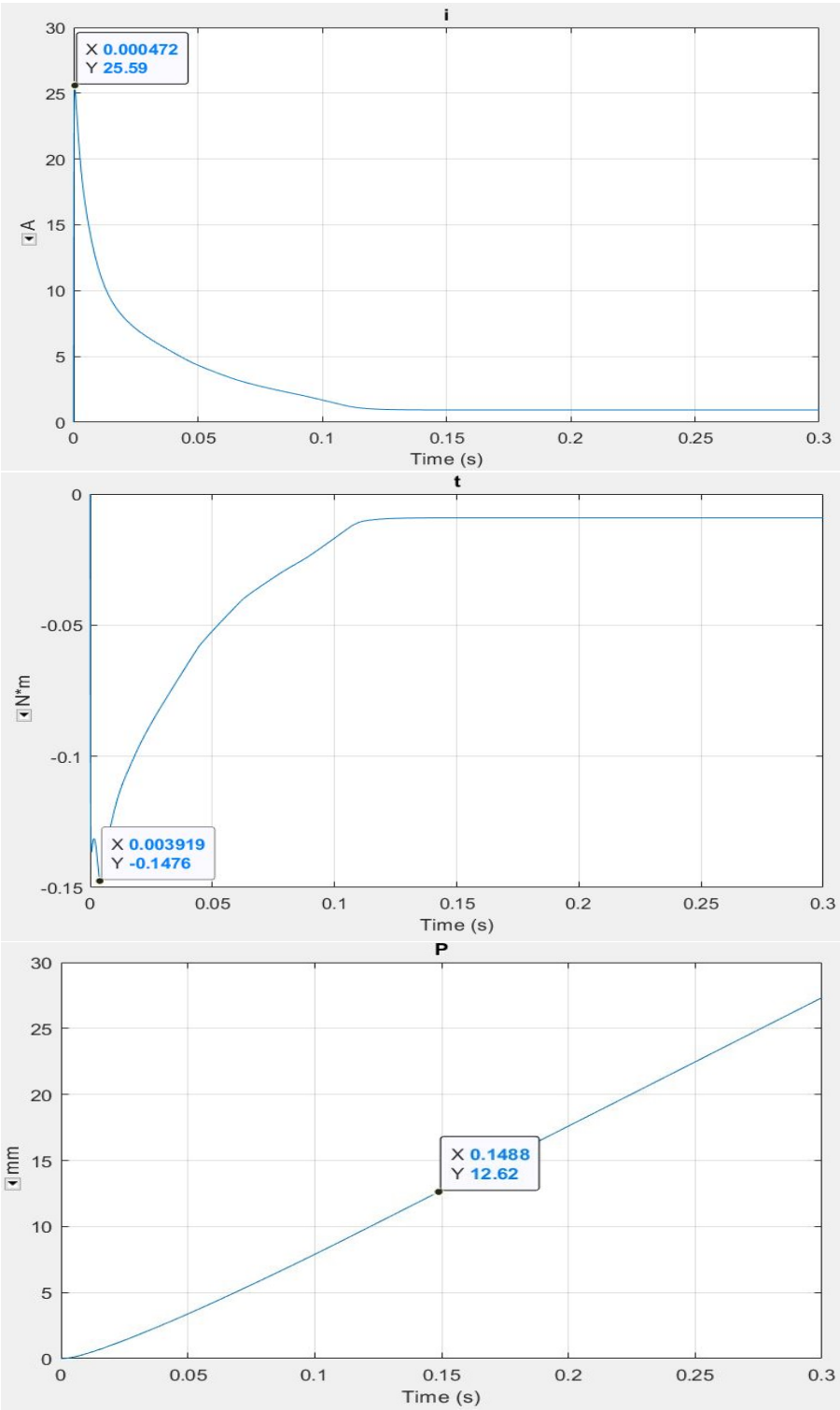

Figure 3.3: Simulation motor current, torque and linear motion in normal operation worst load case

As we can observe, of course average current, peak torque and mean torque increase. The results are quite close to the calculations previously made.
However, looking to the linear motion, it is clear that the motor is sufficiently powerful to win the load in an extremely small period of time, always keeping in mind that here the motion, speed and acceleration profile are not implemented in the simulation.

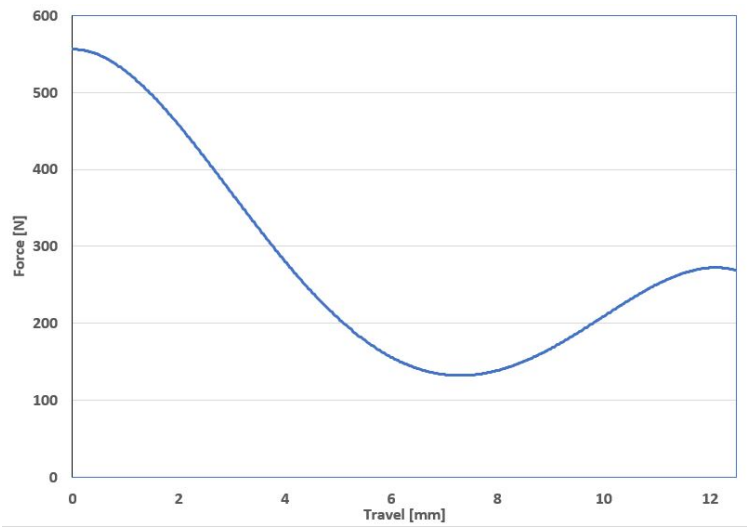

Figure 3.4: Supposed worst case load profile in emergency operation for non linear spring

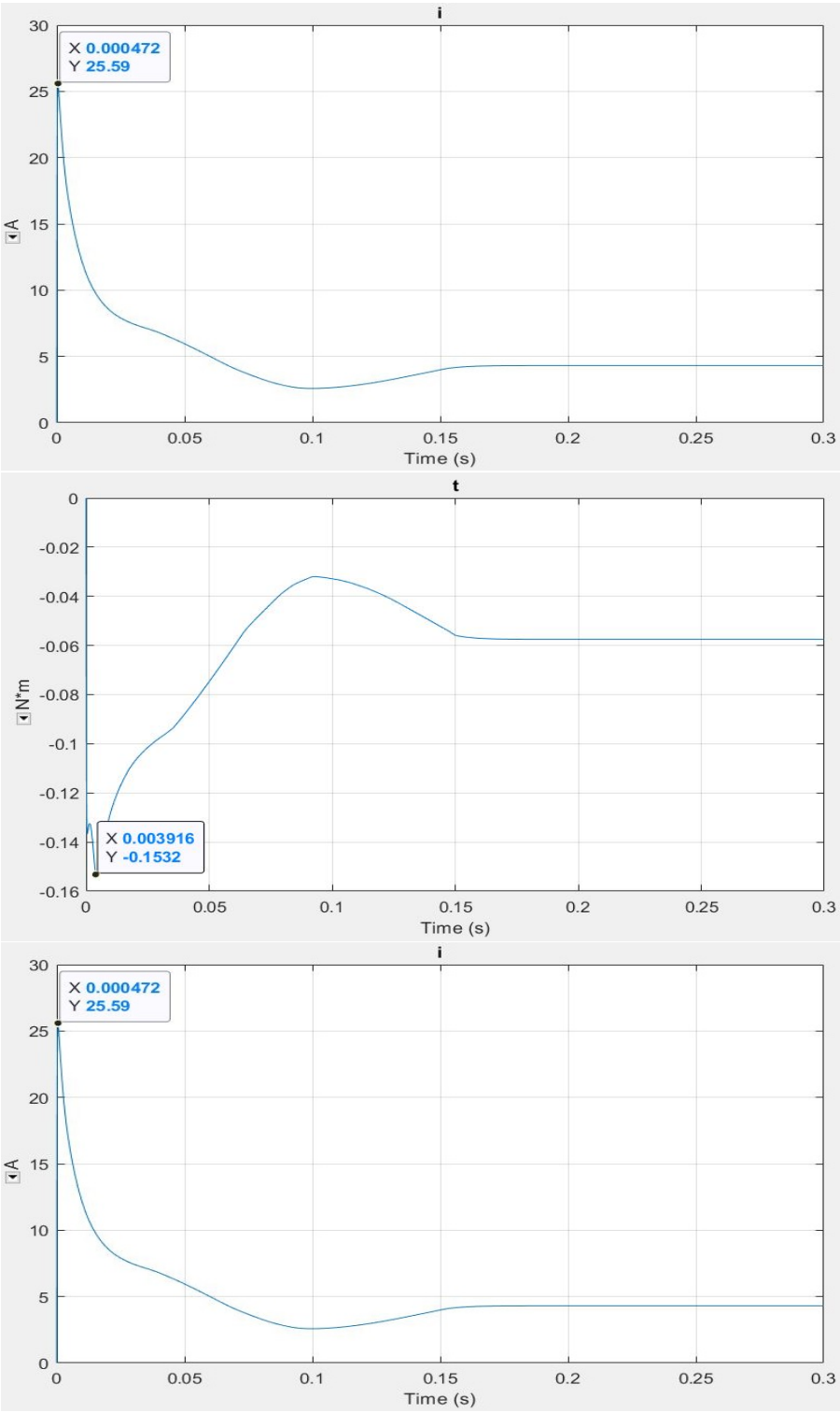

Figure 3.5: Simulation motor current, torque and linear motion in emergency operation worst load case

3.2 Mechanical tests

The process of realization of a shift control system passes through different phases, from the design up to the production. In parallel to the design, is fundamental to have an actual verification of the product, to analyze where the system is strong, and where, instead, is weak: this is done through a testing department, capable of subjecting the product to various verifications and specific tests. The Silatech Srl of Orbassano is provided with a testing laboratory, where it was possible to simulate, even if briefly, the actuator, in order to have some useful data for the emergency unit.
In particular, the tests were carried out to check the calculations, previously showed, made for the emergency spring, fundamental to verify if the emergency system is able to actuate the necessary force.
The actuator that has been used for this phase, was a prototype already realized, without the modifications shown in the previous section but, being the general structure of the reduction gear remained quite similar, the results have been considered reliable.
The prototype that has been realized is represented in figure 3.6.
Passing to the test bench, in the next figures it is possible to see all the components that composed it.
In figure 3.7 it is shown the load recording tools used during the test, that are two load cells: the number one is connected to the right side where the force will be actuated by a linear actuator, while the number two is connected on the reaction side, where we have, theoretically, the load to move.
On the reaction side, have been tested two configurations: one with a reaction spring, one with a 20 and 15 Kg load, as shown in figure 3.9.

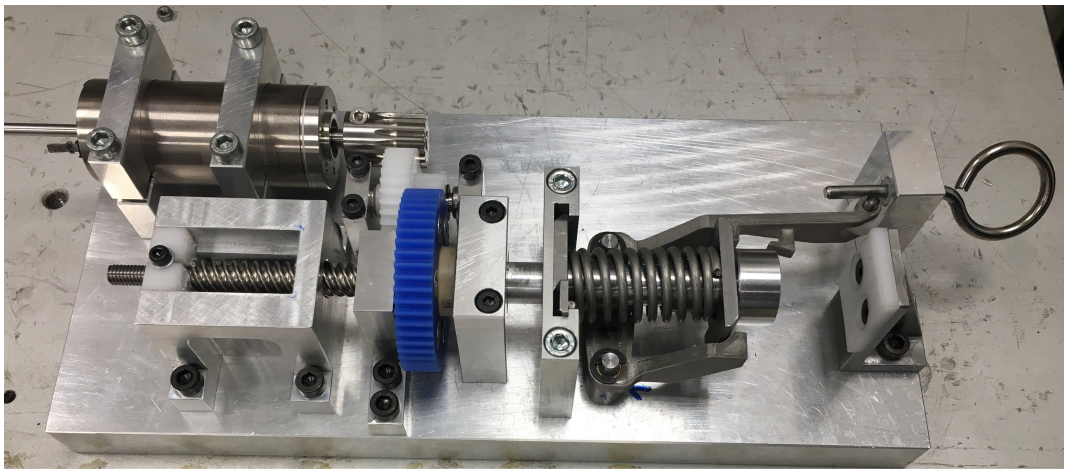

Figure 3.6: Actuator prototype

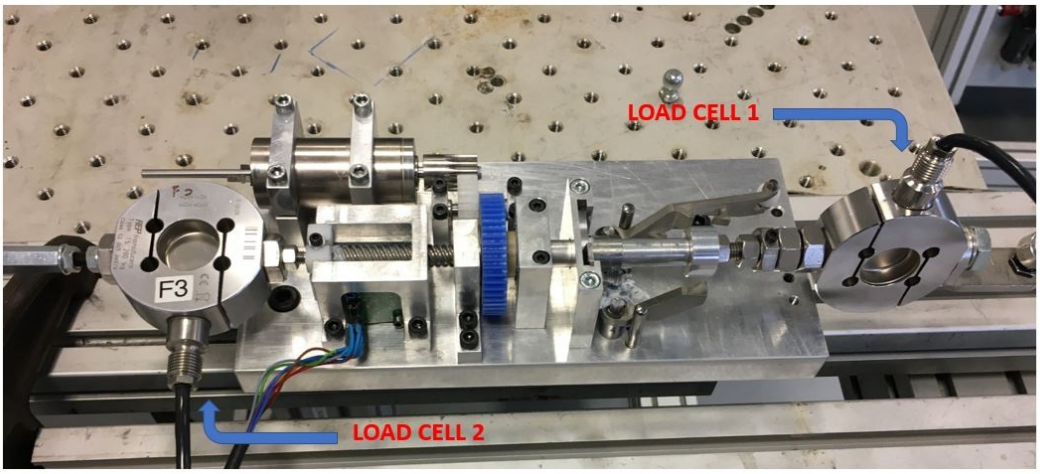

Figure 3.7: Test bench load cells

The actuation force is realized by a linear actuator through a cable, and all the data are recorded by a software installed in a totem, like shown in figure 3.10: the software that is used for the acquisitions it is called Windata, realized and studied by Iridium Italia. In figure 3.8, we have the force application point.

The target of the test is to estimate what could be the losses that we have in the system, considering all the limitations related to a prototype part in which the assembling and all the pieces are realized just to validate and test the design and the functionality of the actuator.

In the first load condition, the spring gives a reaction that is linearly increasing with the travel, which is a condition that is not completely in accordance with the actual case, but that anyway gives some important results: in figure 3.11 it is shown the result obtained in the first test. In green is represented the reaction force, that increases quite linearly with the travel, and in red the cable force applied by the external linear actuator; the force actuation has been set in order to apply a maximum force of 150N, a maximum speed of 5 mm/s and a maximum travel of 12.5 mm: at the maximum applied force, the reaction force is equal to 121 N.

In the second load condition, the load of 15 Kg and the load of 20 Kg simulates a condition of a constant load respectively of 147 N and 196 N: also this condition is not strictly related to the actual case but, recording which is the force to be applied directly to the screw to win that load, we can have the actual maximum value that we need for the emergency spring. Looking to the diagram in 3.12, we have in green the force on the reaction side and in red the applied force through the external linear actuator: the masses apply a force that remains quite constant, except when, due to the motion, are created small oscillations of the masses and friction forces between cable and pulley where the masses are hanging.

However, for both the tests, the maximum applicable force has been increased up

to 300N: where the cable force reaches a stable condition, an horinzontal line, that value of force can be considered as the maximum force to be applied in order to start with the motion of the system.
With respect to the theoretical calculations previously made, the force needed is a little bit greater, but not so far from them: in the spring sizing has been considered a safety factor in order to avoid to have stucking condition due to some unexpected factor(excessive friction, excessive backlash between mechanical parts).
In these tests was not possible to record the travel of the system, data that would be important for the evaluation of the efficiency: to improve the tests reliability, repeatability and accuracy, will be important to implement a standardized test bench, adding the possibility to test the actuator also from the electrical point of view.
The tests have been repeated several times to verify the reliability of the simulations, considering reliable the results obtain through the measuring instruments: the Silatech is a company with several quality certifications necessary to be competitive in the market and, in particular, it is certified IATF (International Automotive Task Force) 16949, a global quality management system standard for the automotive industry; in order to mantain this certifications, for what concerns the testing department, it is necessary to guarantee a certain level of quality of all the measurements: because of this, is mandatory to have all the measuring instruments calibrated periodically to guarantee the precision and the accuracy of the test results.
With a periodical calibration, we can remove the instruments variability, and move our attention on the actual object and on the human factor.
The test has been carried out just at room temperature ($23°C$) but, in order to have a significant evaluation of the system also in extreme conditions, this measurements shall be done also at -40 and $+80°C$, typical temperature cycle used during an endurance test.

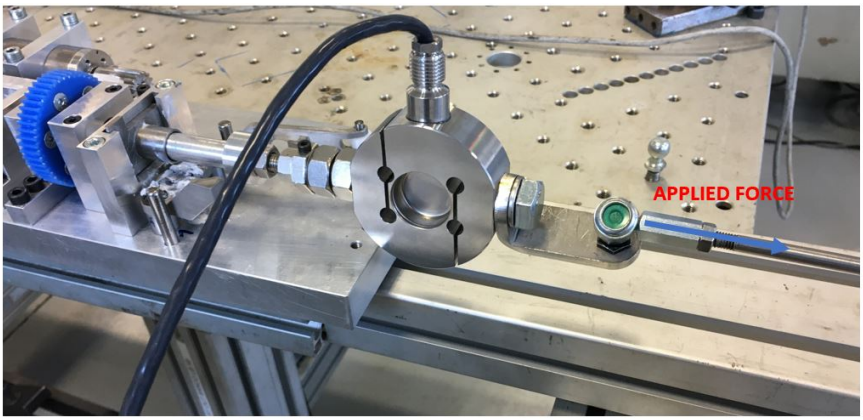

Figure 3.8: Direction of force applied by the external linear actuator

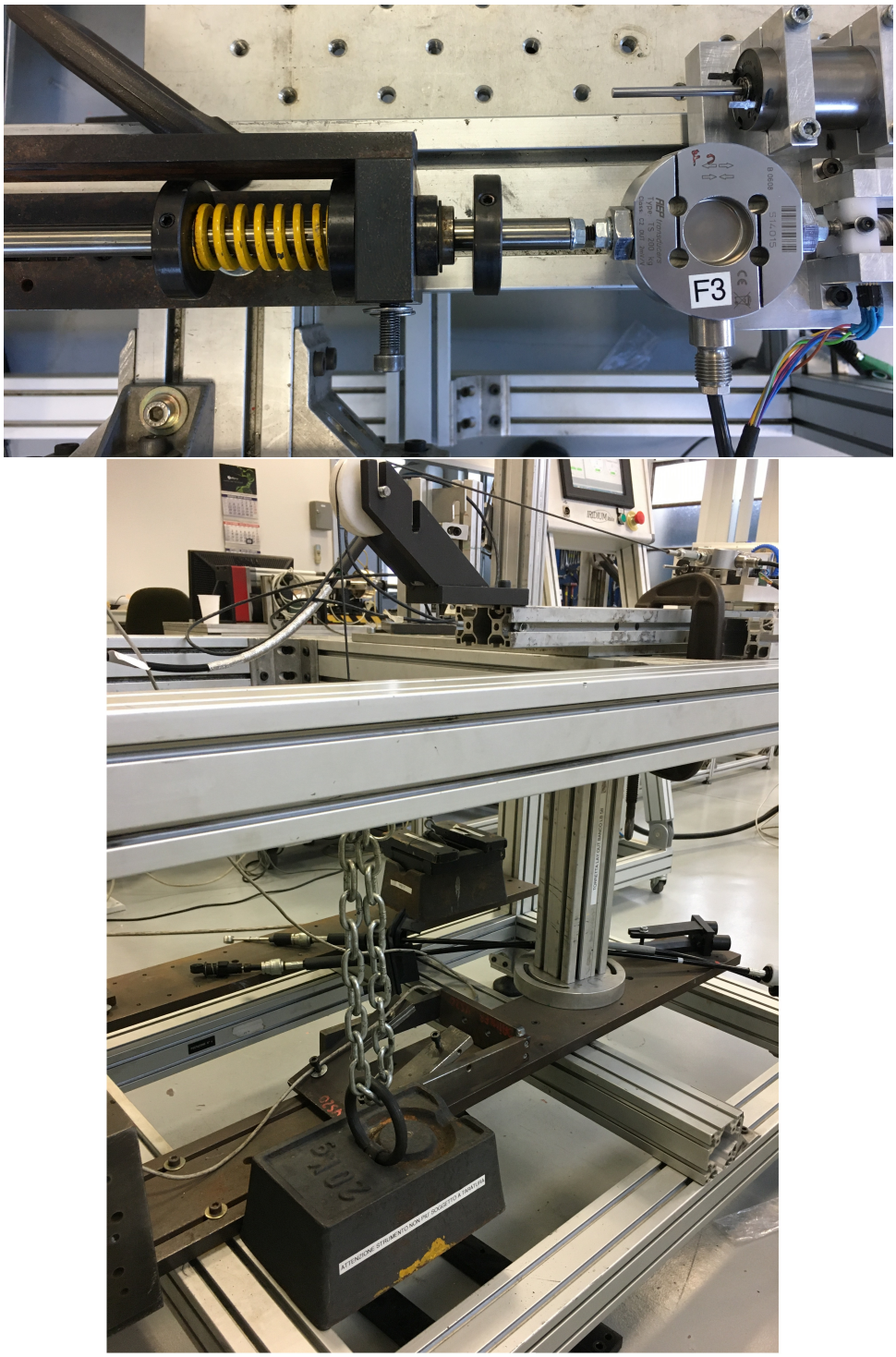

Figure 3.9: From the top: 1)load simulation with reaction spring and 2)load simulation with a mass

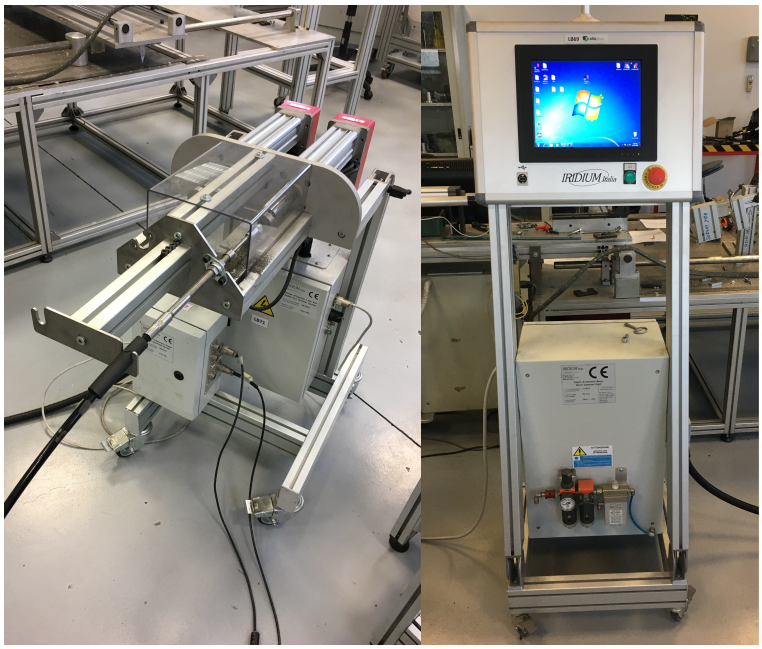

Figure 3.10: Linear actuator and data acquisition totem

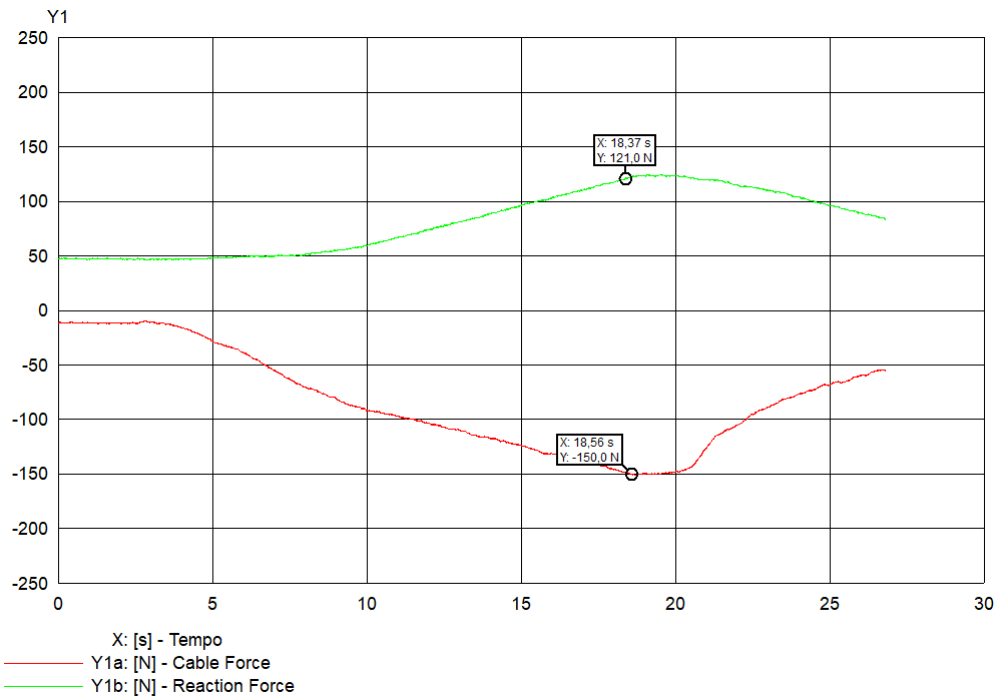

Figure 3.11: Mechanical test with reaction spring

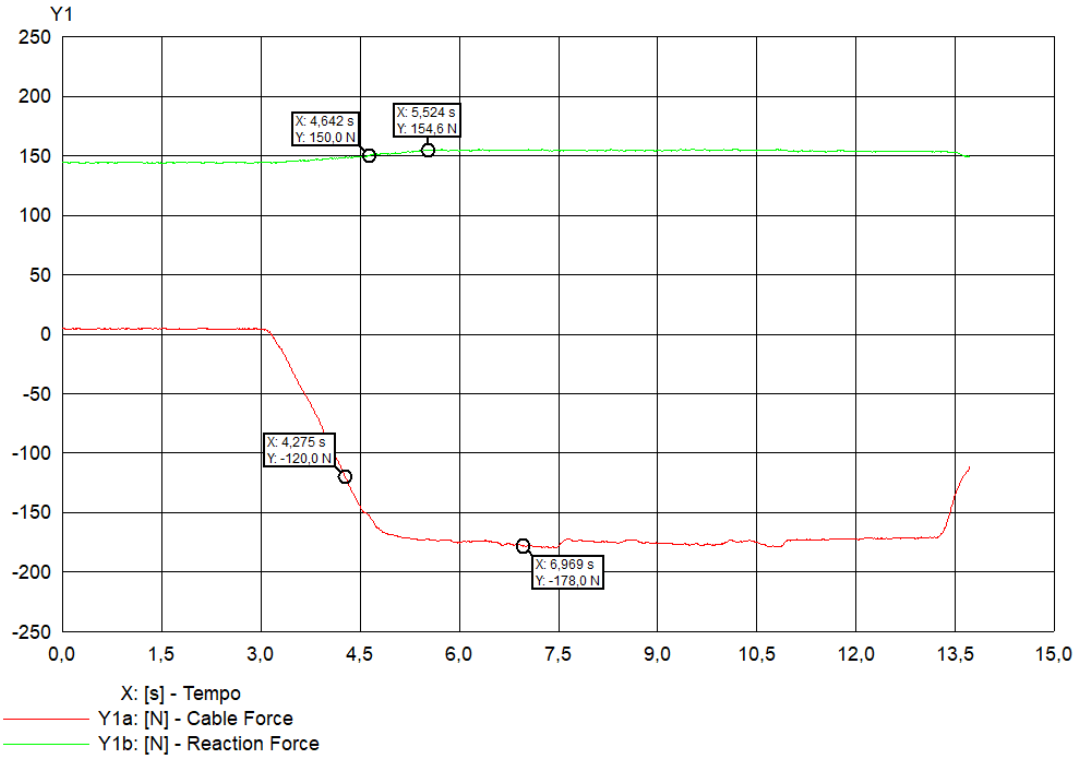

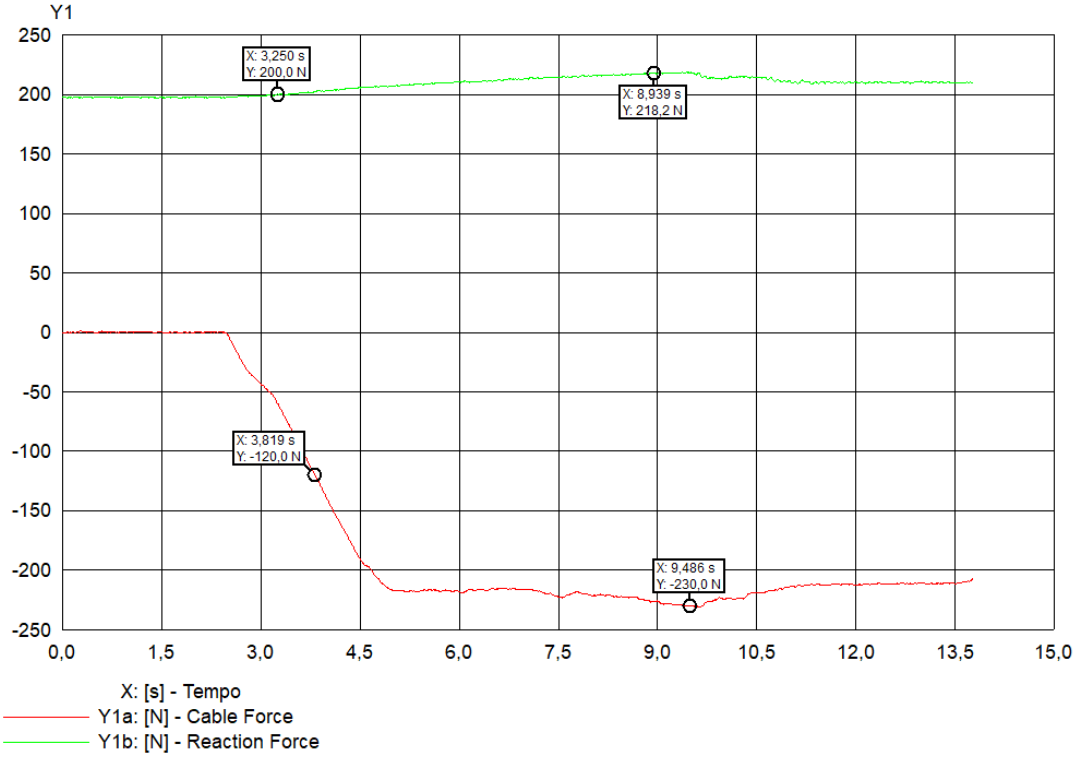

Figure 3.12: Mechanical test with masses: 15Kg and 20Kg

Chapter 4

Possible improvements

On the basis of the obtained results, is now possible to analyze the system macroscopically to identify the weak and strong points of the actuator, trying to find possible betterments.

Starting from the main actuation unit, looking to all the selected motors and to the basic simulations, it is possible to notice how the actuation target is achieved in a smaller period of time with respect to the one analytically imposed: for geometrical constraints, has been chosen , mantaining the use of normal spur gears, to adopt the biggest gear ratio compatibly with the available space; most likely, further increasing the gear ratio would be possible to select a less performant dc motor, always paying attention to the current draw constraints.
The last gear of the reduction system, as previously mentioned, is directly attached to the nut structure in order to apply torque to the nut and provide the motion transformation: for the prototype realization, the solution that has been used is represented in figure 4.1, where the connection is simply realized through bolts, connecting the gear to the nut flange. For the prototype phase, this is possible because we need to have a design validation but, of course, this is not possible for a production object.
A solution could be the co-moulding of the two materials, or obtain the last gear as a single part with the nut using just the nut material: the latter solution in particular, needs a deeper study for materials, task that is also useful to verify alternative materials to be employed in different actuator parts.
The motor used for the calculations, are expensive motors that generally are not used for the production phase of a product, but they are the only available motors on the internet for which it' i easy to obtain all the necessary data fundamental for the calculations. With a deep research, it is possible to reduce the motor cost searching the best trade off between motor performance and gear reduction: for example, passing to a planetary gear reduction system is much more easy to obtain bigger gear ratios with smaller size with respect to normal toothed gears.

The system shall be also studied in terms of structural stresses: through the CAE department of Silatech this could be achieved by means of FEM studies, identifying which are the parts stressed by the static and dynamic forces, based on the required loads. The FEM analysis must be carried out for all the mechanical components and, especially, for the emergency unit, being involved in a safety function.
Speaking about the bearings calculations, there are some topics to be discussed, which were not stuied in depth during the sizing: the bearings interfaces, whose purpose is to study the bearings seats on shaft and housing, the bearing execution, related to bearings internal clearance, preload and tolerances, and finally the bearings sealing, mounting and dismounting. Being a system that must withstands several test cycles, those are technical details that shall be addressed.

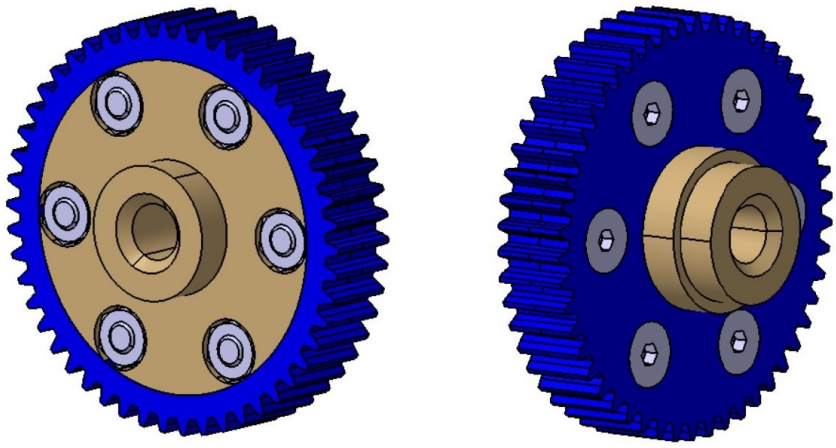

Figure 4.1: Gear and nut mechanical coupling

Passing to the P emergency safety function unit, all the structural part has to be verified: in particular, an in depth analysis will be necessary for the springs and the restraint levers. For the first one, the emergency springs are components that during a vehicle life, hopefully, could be activated a couple of times in case of malfunction, while for the majority of the time will be compressed in the same position: this can create a fatigue stress reducing the effectiveness of the spring and, conseguently, reducing the vehicle safety. For the holding levers, looking to the structure, there are some weak points that must be analyzed to avoid safety issues: in the image 4.2, it is represented a lateral view of the restraint system, and it's clear that due to the shape of the green levers, the bending stress may affect the functionality of the system. If the rotating holding levers are not connected correctly with the rotation pins, the bending can create excessive friction and lock the system. As previously stated, also here the FEM analysis is fundamental.

In the next developments, this part must be modified to make it more robust.
The other important part of the emergency unit is the electromagnet, where a big problem could be the ambient operating temperature.

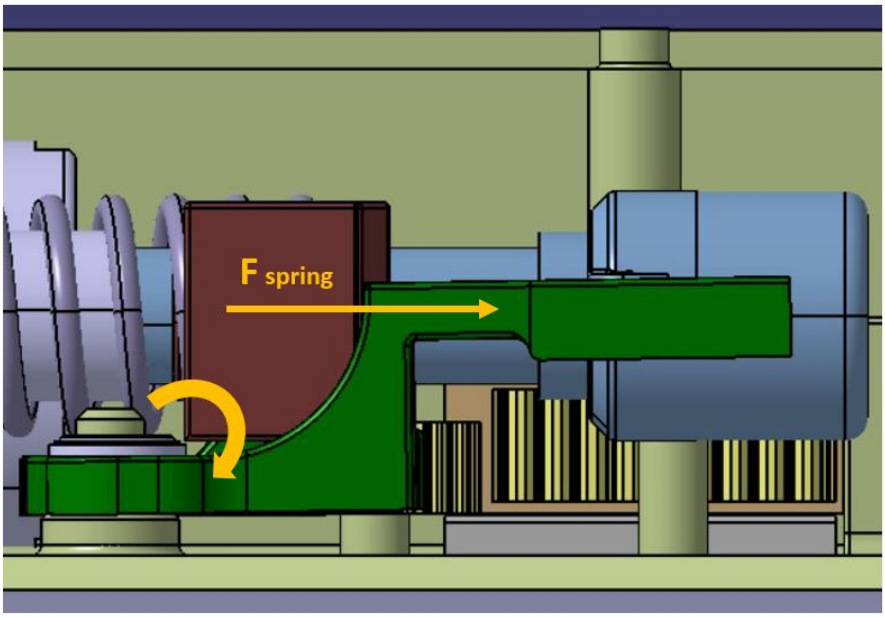

Figure 4.2: Benging moment on the restraint system

The temperature range for which the actuator must be tested is defined by the specification: being a part installed under the shift knob, the temperature profile for which the endurance tests are carried out, ranges from $-40°C$ up to $+80°C$. Being the temperature range sustainable by the electromagnet really close to those of the endurance tests, it is important to be careful to evaluate if is necessary to use heat dissipation systems or special insulations systems.
As mentioned initially, the transmission emergency actuation unit has not been studied in depth in this thesis work: here will be presented a preliminary analysis for the main target of the system and possible improvements with respect to the current configuration.
In figure 4.3 it is represented the lever designed in the starting actuator: the white circle is the trajectory followed by the lever in relation to the rotation point, and it is clear that if the lever has to move for the entire travel (12.5mm) the light blue component (that is rigidly connected with the screw), the rotation that has to cover goes in contrast with the pulley position.
The force applied by the cable, creates a torque around the lever rotation point, and that torque creates a normal force on the light blue component: in the worst case condition, the load is equal to 556.7 N, that correspond to a condition with

the vehicle parked over a slope with 30% of inclination, and with the emergency spring released (500N + 56.7N of spring preload).
The alternative lever shape set for the initial evaluations, it is represented in figure 4.4: this shape is just a representative curve that was not studied, but is comparable with a cam profile, whose study of exchanged forces and curve generation shall be analyzed with the cams theory. In the top image, are also reported the values of the arm of the torque, the distance between center of rotation of the lever and axis of the light blue component and its radius. In figure [17] it is shown how the forces are aplied by the cam on the horizontal surface, and how those forces can create bending moment and friction.
To complete the electromechanical actuator in all its components, also this part must be designed to support the necessary loads and stresses.

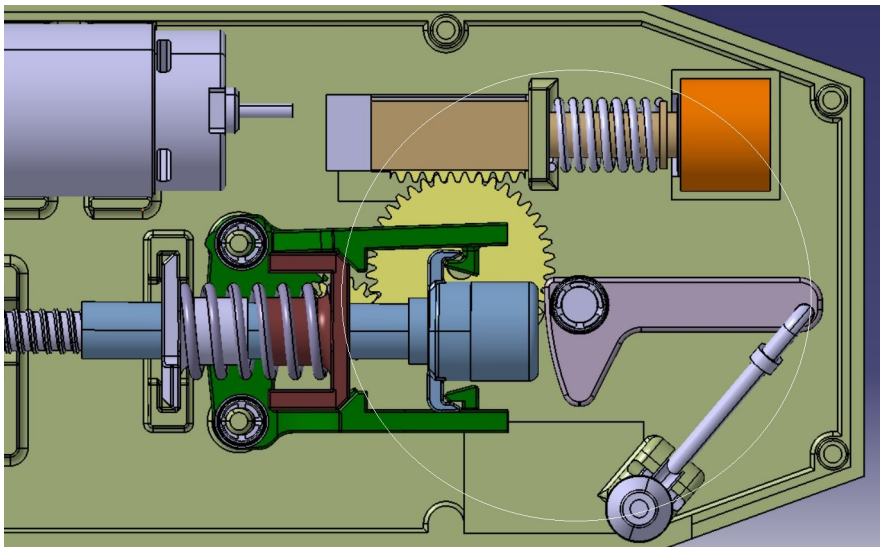

Figure 4.3: Transmission emergency actuation unit, current lever design

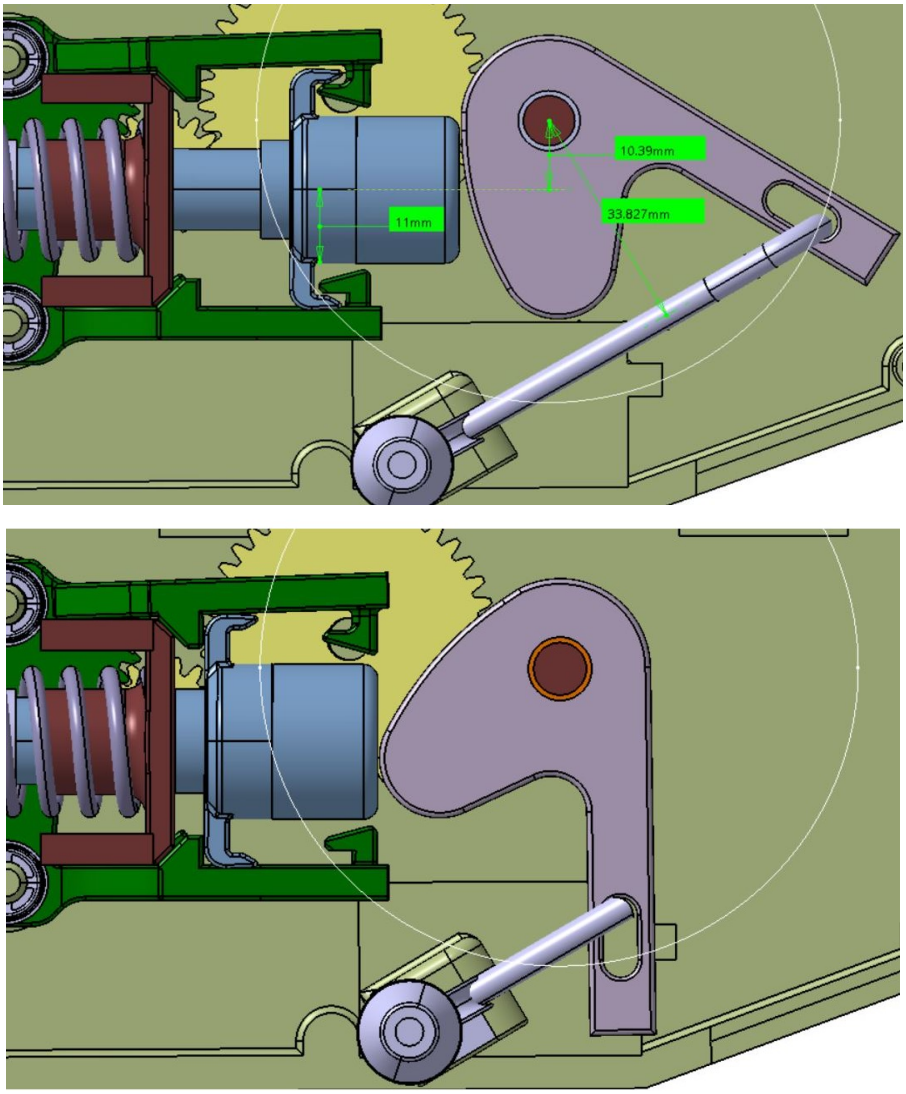

Figure 4.4: Transmission emergency actuation unit, preliminary modified lever design

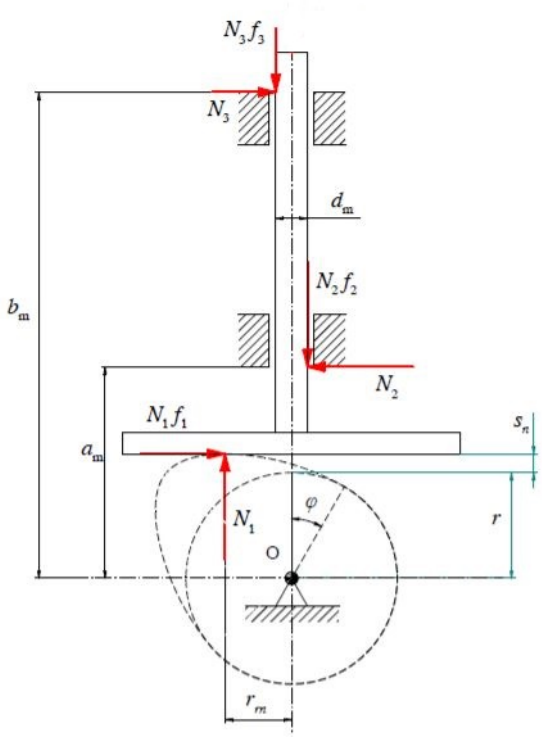

Figure 4.5: Example of exchanged force in a cam mechanism

Chapter 5

Conclusions and outlook

The target of this thesis work, was to figure out a design methodology for an electromechanical actuator, trying to extend the engineering approach to all the parts that make up the system: following the procedure is possible to have an order of magnitude for all the quantities involved in the design phase.
Starting from the customer specifications was possible to, following the outlined procedure, verify the initial actuator configuration: the motor and load coupling is, for an electromechanical actuator, of primary importance, and has been verified how the initial motor and reduction gear were not suitable for the application; then, through the analysis of the worst load cases, have been defined the range of limit conditions that the actuator must undergone, defining for them the important parameters as C_{rms}, C_{peak} and $Dwell\,time$.
After the initial analysis, with the available data, the actual motor and reduction gear selection has been made: with that configuration, a preliminary sizing and verification was carried out for all the components involved in the motion transformation.
Nowadays the safety, in particular in automotive field, is of primary importance: the peculiar emergency function presented in the actuator, has been modified in order to be closer to the customer specification requirements, adding also the sizing and verification of the safety springs. These mechanical energy storage devices must guarantee always the activation of the safety function, for this reason this actuator section must be tested also in severe ambient conditions. Finally, the system has been simulated using initially a simple Simscape model that was useful as a first verification for the motor and reduction gear selection, in particular for the peak values of torque, speed and current absorption. Then, for the emergency part, the realized prototype has been physically tested to verify the necessary force to move two kind of load, one with reaction spring on the actuation side, and one with two masses (15 and 20 Kg) directly attached to the output screw: this was extremely useful in order to have a comparison for the spring calculations previously made. The obtained results, have confirmed the order of magnitude of the calculations.

The presented system opens up to several possible future developments: in addition to the possible improvements presented in the previous chapter, for what concerns all the simulations reported up to now, have been useful just for the evaluation of peak torques required by the system, but they are not sufficiently detailed to estimate the actual actuator behavior in dynamic conditions; it would be useful to implement a control strategy in order to have a model that is reliable, adding the possibility to have always a first verification and validation of the designed system. For the control strategy in the actual field, it would be also really interesting a focus on the measurements sensors, finding the most suitable for the system working conditions: optical, magnetic, inductive transducers, generally linears, or encoders, rotative sensors directly on the motor stator.
Looking to the emergency system, the electromagnet is a component that for variable temperature environment can creates functional problems and being related to an emergency function the faults are not allowed: therefore, that part of the actuator must be study for a robust design, improving the reliability of the same electromagnet or trying to find suitable alternatives.

The electromechanical actuators in the mechanical, automotive and many other sectors, are extremely spread systems that probably will replace pneumatic and hydraulic actuators: being able to identify the right guidelines quickly and intellingently can lead to today's market advantage.
The complete design of a product like the one covered in this thesis work, requires a huge amount of effort, time and attention to the details: the development carried out so far does not claim to be representative of a final product, it is not enought to guarantee an object ready for the use and for the production; instead, is important to continue the development in order to guarantee, step by step, an increasingly more precise, accurate, reliable and performing product.
The development of this system shall continue, step by step, trying to find economically competitive solution with an engineering perspective.

Bibliography

[1] Volkswagen. *The 02E Direct Shift Gearbox*. 2004.

[2] Guan Qiao et al. "A review of electromechanical actuators for more all electric aircraft systems". In: December (2017).

[3] M. Budinger et al. "Optimal preliminary design of electromechanical actuators". In: 228.9 (2014), pp. 1598–1616.

[4] M. Budinger et al. "Estimation models for the preliminary design of electromechanical actuators". In: 226.3 (2012), pp. 243–259.

[5] R.Adamini D.Tosi G.Legnani M.Tiboni. *Meccanica degli azionamenti*. 2016.

[6] Igus. *Dry-tech linear systems and ball bearings*. 2017.

[7] S. Cinquemani. *Functional Mechanical Design*. 2015.

[8] A. Gasparetto. *Meccanica applicata alle macchine*. Chap. 6.

[9] T.Raparelli C.Ferraresi. *Meccanica applicata*. 2015.

[10] L. Biagiotti C. Melchiorri. *Trajectory Planning For Automatic Machines and Robots*. 2008.

[11] L. Galgani A. Carati. *Meccanica razionale*. 2008. Chap. 1.

[12] E. Brusa T. Berruti. *Elementi di Costruzione e disegno di macchine, Lessons notes*. 2015.

[13] Kohara Gear Industry. *Gear technical reference: the role gears are playing*. 2018.

[14] SKF. *Rolling bearings: Principles of rolling bearing selection*. 2018.

[15] SKF[online]. *skf.com/bearing calculator*. 2019.

[16] Red Magnetics. *Red magnetics catalogue*. 2019.

[17] Iryna Hren et al. "Analysis of torque cam mechanism". In: *MATEC Web of Conferences* (2018).